



HAL
open science

Topological point defects in nematic liquid crystals

Maurice Kleman, Oleg D Lavrentovich

► **To cite this version:**

Maurice Kleman, Oleg D Lavrentovich. Topological point defects in nematic liquid crystals. Philosophical Magazine, 2006, 86 (25-26), pp.4117-4137. 10.1080/14786430600593016 . hal-00513663

HAL Id: hal-00513663

<https://hal.science/hal-00513663>

Submitted on 1 Sep 2010

HAL is a multi-disciplinary open access archive for the deposit and dissemination of scientific research documents, whether they are published or not. The documents may come from teaching and research institutions in France or abroad, or from public or private research centers.

L'archive ouverte pluridisciplinaire **HAL**, est destinée au dépôt et à la diffusion de documents scientifiques de niveau recherche, publiés ou non, émanant des établissements d'enseignement et de recherche français ou étrangers, des laboratoires publics ou privés.



Topological point defects in nematic liquid crystals

Journal:	<i>Philosophical Magazine & Philosophical Magazine Letters</i>
Manuscript ID:	TPHM-05-Oct-0434.R1
Journal Selection:	Philosophical Magazine
Date Submitted by the Author:	14-Jan-2006
Complete List of Authors:	Kleman, Maurice; Université Pierre-et-Marie-Curie, IMPMC Lavrentovich, Oleg D; Kent State University, Liquid Crystal Institute
Keywords:	topological theory of defects, liquid crystals, point defects
Keywords (user supplied):	



Topological point defects in nematic liquid crystals

MAURICE KLEMAN*‡ and OLEG D. LAVRENTOVICH†

‡Institut de Minéralogie et de Physique des Milieux Condensés (CNRS UMR 7590),

Université Pierre-et-Marie-Curie, Campus Boucicaut, 140 rue de Lourmel, 75015 Paris, France

†Chemical Physics Interdisciplinary Program and Liquid Crystal Institute, Kent State University,

Kent, Ohio 44242, USA

Abstract

Point defects in nematics, also called hedgehogs, are topological entities that have no equivalent in ordered atomic solids, despite the homonymy. They have been the subject of intense experimental and, above all, theoretical (analytic and computational) investigations in the last thirty years. They are present in bulk specimens and at the specimen boundaries. This review article stresses the importance of the core structure of the defect, of its possible splitting into a disclination loop, of the boundary conditions, and takes stock of the recent advances on point defects in nematic colloidal suspensions. An important topic is the formation of strings between opposite hedgehogs (radial and hyperbolic), and their role in the dynamic properties of nematics.

Keywords: liquid crystals, point defects, hedgehogs, boojums, topological defects

1. Introduction

A nematic liquid crystal is an anisotropic fluid formed by rod-like or disk-like molecules that tend to be parallel to a common direction, the *director*, noted \mathbf{n} ($n^2=1$). The directions \mathbf{n} and $-\mathbf{n}$ are physically equivalent: $\mathbf{n} \equiv -\mathbf{n}$. There is no long-range translational order in the system and thus nematics are fluid and very sensitive to the external field, which explains why they became a key technological material in applications such as informational displays. Nematic liquid crystals are in the focus of intensive interdisciplinary studies also because they represent a well-defined soft matter system with a rich variety of supramolecular structures, most notably those corresponding to the so-called topological defects. A topological defect is a configuration of the order parameter that cannot be transformed continuously into a uniform

1
2
3 state. They can occur during the symmetry breaking phase transitions, under an external
4 field, or simply be a necessary element of an equilibrium state. For example, in a sufficiently
5 large spherical nematic droplet with perpendicular alignment of molecules at the surface, the
6 director field forms a radial-like configuration with a point defect at the centre, in order to
7 reach an equilibrium state. This point defect in the director configuration is of a completely
8 different nature as compared to point defects such as vacancies and interstitials in solid
9 crystals [1]; its topological nature means that the distortions of the order parameter around the
10 “point” extend throughout the entire system.
11

12
13
14
15
16
17 The singular points of a *vector field* (cols, nœuds, foyers, etc) were classified by
18 Poincaré [2], by using the tools of the theory of ordinary differential equations; Nabarro[3]
19 was the first to notice that Poincaré’s method can be applied, with the purpose of classifying
20 point defects, to spins in a ferromagnet and directors in a nematic insofar as the sample does
21 not show circuits along which \mathbf{n} is reversed.
22

23
24
25
26 The *topological classification* of defects, on the other hand, relies on the topological
27 properties of the *order parameter space*. It does not give a classification as detailed as the
28 vector field one, but its principles can be extended to any ordered medium and to defects of
29 any dimensionality [4,5]. The scalar order parameter $S(T)$ of a uniaxial nematic is the
30 thermal mean $\frac{1}{2} \langle (3\cos^2 \theta - 1) \rangle$ of the orientation of the molecules about the director. More
31 precisely, the order parameter (o.p.) is a traceless tensor $Q_{ij} = S(T)(n_i n_j - \frac{1}{3} \delta_{ij})$. The o.p.
32 space is the space of all the realizations of the o.p.. In the case of a uniaxial nematic, a sphere
33 of unit radius represents adequately all the directions of \mathbf{n} ; the o.p. space is therefore a *half*
34 sphere, namely the *projective plane*, noted P_2 , see [6]. Topological defects of various
35 dimensionalities d in ordered media are classified by the homotopy groups $\Pi_n(V)$, $n = D - d -$
36 1 , where D is the space dimension; in a 3D nematic, $V = P_2$, $n = 1$ stands for line defects
37 (disclinations), $n = 2$ for point defects. The topological charge (an invariant) carried by a
38 point defect can be calculated by the relation [7]
39

$$4\pi N = \iint \varepsilon_{ijk} \varepsilon_{pqr} n_q \cdot j n_{r,k} n_p dS_i \quad (1)$$

40
41
42
43
44
45
46
47
48
49
50
51
52
53 where the integration is performed on a sphere-like surface surrounding the singular point. N
54 is an integer; $\Pi_2(V) = Z$. Point defects $N = \pm 1$, the only ones ever observed experimentally,
55 are called *hedgehogs*. Because Eq. 1 is odd in the director components and $\mathbf{n} = -\mathbf{n}$, the same
56 point defect can be assigned opposite charges: also, the charge can be drawn opposite by a
57 circumnavigation of the point defect around a disclination line of strength $k = \pm \frac{1}{2}$ (about
58
59
60

which the director changes sign) [8]. It is usual to assign the value $N=+1$ to a radial hedgehog, $N=-1$ to a hyperbolic hedgehog, see Fig. 1. Nabarro has probably been the first to show a keen interest in the topology of defects in a nematic [9] by noticing that the Euler-Poincaré characteristic of a sphere [5] measures the total strength of the disclinations piercing the boundary of a nematic droplet, if the boundary conditions are such that the director is everywhere parallel to the droplet surface ($\sum_i k_i = 2$).

Fig. 1. Capillary tube with homeotropic (*i.e.* normal) boundary conditions, meridian section. The director is in the meridian plane. Point defects $N = +1$ (radial hedgehog) and $N = -1$ (hyperbolic hedgehog).

The free energy density associated with the changes of the tensor order parameter in the vicinity of the nematic-isotropic phase transition is of the Landau-De Gennes form:

$$f_{LDG} = \frac{1}{2}a(T, p)\text{tr} Q^2 - \frac{1}{3}b\text{tr} Q^3 + \frac{1}{4}c(\text{tr} Q^2)^2 \quad (2)$$

When the scalar order parameter does not change much, which is true for director deformations over the scales much larger than the molecular size, then the free energy density of the elastic director distortion is written as the Frank-Oseen expression

$$f_{Fr} = \frac{1}{2}K_1(\text{div} \mathbf{n})^2 + \frac{1}{2}K_2(\mathbf{n} \cdot \text{curl} \mathbf{n})^2 + \frac{1}{2}K_3(\mathbf{n} \times \text{curl} \mathbf{n})^2 - K_{24} \text{div}(\mathbf{n} \text{div} \mathbf{n} + \mathbf{n} \times \text{curl} \mathbf{n}) \quad (3)$$

with Frank elastic constants of splay (K_1), twist (K_2), bend (K_3), and saddle-splay (K_{24}).

Nabarro made also very early observations of hedgehogs in capillaries [10]. In fact, there have been very few detailed experimental investigations of hedgehogs in the course of time since their appearance in the realm of nematics, compared to the flourishing of theoretical studies, these latter encouraged by the development of computer methods. On the other hand, theory and experiment seem to go hand in hand for point defects in colloidal suspensions in nematics, where an air bubble (which acts as a positive $N=+1$ point defect) or a droplet or a particle that compensate a negative $N=-1$ point defect in their vicinity [11], can form a stable dipole.

This paper presents a brief review of bulk point defects (hedgehogs) and surface singular points, often called boojums (the name is due to Lewis Carroll and has been adopted frenetically by the superfluid and liquid crystal communities thanks to Mermin).

2. Bulk and surface singular points.

2. 1. Static observations

1
2
3 Defects usually appear in the bulk of a sample by symmetry breaking, at the
4 isotropic→nematic transition T_{IN} , either by a thermal quench or a slow transition; pressure
5 quench has also been employed. One expects to get this way a random array of defects of
6 various dimensionalities: point defects, disclination lines, and configurations or solitons (non-
7 singular topological defects) [4]. The final defect distribution depends on the time of
8 annealing and on the boundary conditions, *i.e.* on the *anchoring* conditions at the boundaries
9 of the sample, like those induced by a physical or chemical surface treatment; this forces the
10 orientation of the molecule.
11
12
13
14
15
16
17

18 We are interested in *point defects*. A remarkable experimental result is that their
19 occurrence *in the bulk* just after quench (independently of the boundary conditions) is a rather
20 rare, if ever observed, event [12]. It has been given of this phenomenon an interesting (and
21 subtle) explanation [13]. The topological charge N (Eq. 1) measures twice the number of
22 times that P_2 is covered by the order parameter (the director); this is a rather difficult
23 geometric requirement to be obeyed by the correlated nematic domains which appear
24 randomly about some point of the sample at the transition. The probability of this event can
25 be calculated [13]. The idea follows the lines of the celebrated Kibble mechanism for the
26 generation of cosmic strings (considered as singularity lines) in the early universe [14], which
27 has inspired laboratory experiments on liquid crystals, see *e.g.* [15].
28
29
30
31
32
33
34
35

36 Hedgehogs are thus observed in special geometries with specific anchoring conditions,
37 namely in *capillaries* [10,16,17,18,19], in nematic *droplets* [20], and in confined parallel
38 samples with *hybrid boundary conditions* [21,22]. Our references are not exhaustive. On the
39 other hand, hedgehogs are the rule rather than the exception, in nematic colloidal suspensions
40 (see next section), but this also proceeds from the special anchoring conditions met in such
41 systems.
42
43
44
45

46 In capillaries with homeotropic anchoring, the molecules normal to the boundaries
47 force a radial geometry, as pictured in Fig. 1; one observes that the director ‘escapes along the
48 3rd dimension’ –namely the axis of the capillary– as nicely worded by Meyer [23]. The
49 $k = +1$ disclination forced by the boundary conditions is therefore continuous along its core
50 (or, differently stated, coreless). Observe that the escape is either up or down, with equal
51 probabilities if the normal anchoring is perfect. Thus two types of point defects do appear, of
52 opposite charges $N = \pm 1$. The director configuration can be investigated experimentally by
53 polarized light microscopy; the resulting observations satisfy the expected geometry, at least
54 qualitatively –this experimental method does not bring a large resolution. Therefore the role
55
56
57
58
59
60

played by the anisotropy of the elastic moduli K_1, K_2, K_3 in the director configuration around the hedgehogs [23,24] has not yet been satisfactorily tested.

Fig. 2. Schlieren texture in a sample with degenerate planar anchoring conditions. The sample is observed between crossed polars. There are two black brushes associated with the $k = \pm 1/2$ lines, and four brushes (the Maltese cross) associated with the $k = \pm 1$ lines.

This same anisotropy is also responsible for the configuration of the director about $k=+1$ disclination lines, but also about $k=-1$ lines; see [25]. Disclination lines can be observed end-on in well-annealed nematic samples formed between two flat glass plates (Schlieren textures, see Fig. 2). Topology requires that the sum total of the disclination charges vanishes, $\sum_i k_i = 0$. One observes $k = \pm 1/2$ and $k = \pm 1$ lines. In most experimental cases, in particular SMLCs (small molecule liquid crystals) the escaped geometry is stable with respect to planar singular $k = \pm 1$, and point defects are present; the situation is more involved in main chain PLCs (polymer liquid crystals) where usually the splay modulus is so large that the escape can be absent in a radial geometry [26]. Thus, apart a few exceptions, there is ample evidence that the integer lines are coreless and carry point defects, often located outside the sample. Monte Carlo calculations have confirmed these results [27].

The topology of a droplet with homeotropic anchoring is compatible with a radial hedgehog, but its actual presence depends on the anchoring energy $\sim W\delta^2$ (which measures the excess surface energy necessary to turn the director apart the normal direction by an angle δ , W is called the surface anchoring coefficient), and the droplet size R . Compare the surface energy, which scales as WR^2 for a uniform director, and the bulk energy, which scales as $(K/R^2)R^3 = KR$ for a radial hedgehog; it is easy to convince oneself that in a droplet of radius R smaller than approximately $R_c = K/W$ the director is uniform, whereas a larger droplet contains a radial hedgehog [4].

In a droplet with planar (degenerate) anchoring, the director field should obey the Euler-Poincaré theorem [6,9] and, accordingly, must suffer either two singularities with $k=1$ or one singularity with $k=2$. The first case (two $k=1$ singularities) is often met when a nematic droplet is suspended in an isotropic fluid such as glycerol, say [28, 20]; the second one being more specific of biaxial nematics (for the existence of which there appears to be new experimental evidences [29,30]). Note that in both cases the point defects are essentially surface defects that cannot move inside the nematic bulk because of the boundary conditions. They are thus different from the hedgehogs that can exist both in the bulk and at the surface. Because of this distinction, these surface defects are called boojums [31]; a necessary

condition for their formation is that the director field is either tangential or tilted with respect to the surface so that the defect is characterized by an invariant k in addition to N [20].

Finally, hybrid samples: a typical example is when a thin nematic film is spread onto the surface of an isotropic fluid at which the director is oriented tangentially (planar degenerate alignment) whereas the upper boundary is free. Quite often the spontaneous anchoring at the nematic-air interface is homeotropic or tilted. The competition between the two anchoring modes is relaxed by the presence of surface point defects [21,22].

2.2. Theory of the static point defect.

In the *one-constant* approximation (*i.e.* $K = K_1 = K_2 = K_3$) the geometry of a point defect can be represented near its core by the equations

$$\phi = N\theta_r + \phi_0, \quad \tan \frac{\theta}{2} = \left(\tan \frac{\lambda}{2}\right)^N \quad (4)$$

where θ , ϕ are spherical angles for the director in \mathbf{r} ; θ_r the polar angle of \mathbf{r} in the horizontal plane, λ the angle between the Oz axis and the direction \mathbf{r} [17]. It is apparent that $\theta = +\lambda$ for the star-like radial hedgehog, $\theta = -\lambda$ for the hyperbolic hedgehog. The energy does not diverge on the core; one gets, for the radial hedgehog, by integrating the free energy density all over a ball of radius R with a point defect at the centre

$$E_1 = 8\pi KR \quad (5a)$$

and

$$E_{-1} = \frac{1}{3}8\pi KR \quad (5b)$$

for the hyperbolic hedgehog [32].

Of course, there is a physical core, where the nature of the order parameter is modified with respect to the region of 'good' crystal. Let us write for the radial hedgehog the total energy as

$$E_1^{tot} = 8\pi K(R - r_c) + \gamma r_c^3 \quad (6)$$

Minimizing this expression, one gets

$$r_c = \sqrt{8\pi K/3\gamma}; \quad E_1^{tot} = 8\pi K\left(R - \frac{2}{3}\sqrt{8\pi K/3\gamma}\right) \quad (7)$$

r_c does not depend on the size R of the sample, and the energy is not significantly different from E_1 , if the core is microscopic compared to R , as expected. Therefore one can adopt E_1 as a first approximation for the total energy.

To find the minimizer of the integral $\frac{1}{2} \int (\nabla \mathbf{n})^2$ (one-constant approximation) in a given volume $U \subset \mathbf{R}^3$ is a problem relevant to the theory of harmonic maps with defects [33]. An interesting result is that the minimal energy $E_{\cup\{i\}}$ of a set $\cup\{i\}$ of given point defects $\{i\}$ with $N_i = \pm 1$, such that $\sum N_i = 0$, is given by the expression

$$E_{\cup\{i\}} = 4\pi KL \quad (8)$$

where L is the minimal total length of the dipoles formed by linking point defects of opposite signs two by two. One cannot overestimate the physical importance of this result that stresses the interactions between opposite hedgehogs. These dipoles are indeed visible in Schlieren textures. A somewhat analog result was obtained in [34,35] through a dimensional analysis, but for a unique pair.

Experimental observations show that the real situation is somewhat more complex, even if some results of the simple model above do subsist: a)- K_2 is always small compared to the other moduli; it is then expected that the radial symmetry could be broken by a twist deformation. This phenomenon has been observed for surface defects-boojuims in Schlieren textures of lens-shaped droplets [36] and for radial hedgehogs in droplets [28], and studied later for spherical bipolar droplets with pairs of boojuims at the poles, both experimentally [20,37] and theoretically [38,39]; in relation with these investigations, a radial hedgehog is *not* a minimizer in a ball with homeotropic conditions, if the Frank constants are anisotropic [40]; b) as pointed by Press and Arrott [36], the structure of defects is influenced by the splay-cancelling mechanism, according to which the energy of splay deformations along one direction can be *reduced* by splay in another direction, somewhat similar to the phenomenon of soap films adopting a catenoid shape; c)- it has been suggested by Melzer *et al.*, on the basis of their observations [10], that point defects might be split into disclination loops, of strength $k = +\frac{1}{2}$ for a radial hedgehog, of strength $k = -\frac{1}{2}$ for a hyperbolic hedgehog, Fig. 3.

Fig. 3. Splitting of point defects into disclination loops: a)- $N = 1 \equiv k = 1/2$; b)- $N = -1 \equiv k = -1/2$

Two *theoretical* elements have been put forward which complete the present picture of point defects in nematics a)- the divergence moduli K_{13} , K_{24} can play a role in the stability of the model, in particular might decide whether the point defect is split, or not, into a disclination loop; b)- the order parameter might change smoothly in the core region, not only in modulus, but also in character. It has indeed been suggested that it might be biaxial [41]. Computer calculations validate this suggestion. We comment on these two points.

The Frank-Oseen elastic theory in the director representation has been used in [42] and [43] to compare the energies of the hedgehogs and their disclination loop modifications. The divergence elastic term K_{24} is introduced in [43]. Eq. 5a, 5b become

$$E_{+1}^{tot} = 8\pi(K - K_{24})(R - r_c) + \gamma r_c^3 \quad (9a)$$

for a radial hedgehog, and

$$E_{-1}^{tot} = \frac{1}{3} 8\pi(K + K_{24})(R - r_c) + \gamma r_c^3 \quad (9b)$$

for a hyperbolic hedgehog. The transformation to a disclination loop of radius ρ adds in both cases a term of the order of ρK_{24} . It is clear that in the frame of this simplified model the $k = \frac{1}{2}$ loop is forced to expand if $K_{24} < 0$, to shrink if $K_{24} > 0$, the reverse being true for the $k = -\frac{1}{2}$ loop. The radius of the loop stabilizes for a value $\rho \sim \xi \exp\left(-\frac{4K_{24}}{K}\right)$, which is microscopic (ξ is the nematic coherence length). By applying the electric field perpendicular to the loop in a nematic material with a positive dielectric anisotropy, one can expand the loop to a larger radius [44]. See [45] for a recent calculation of the hyperbolic hedgehog in the same vein, but using the full Frank moduli anisotropy.

For the study of the core itself, the Landau-de Gennes theory has been largely employed, allowing a variation of the scalar order parameter. It is shown in [46] that spherically symmetric configurations are exact solutions which minimize the Landau-de Gennes free energy, and that the core, whose size is found large compared to ξ , is isotropic. But disclination loops are also solutions. A number of papers [47,48] have exploited with success the suggestion that the core of a $|k| = \frac{1}{2}$ line is biaxial [41,49,50].

Complete models with anisotropic coefficients, divergence elastic terms, Landau expansion in the full free energy, to what has to be added the role of boundary conditions at a finite distance, produce more complicated results, see *e.g.* [51,52]. Of course, these new developments often require heavy computational methods, see [53].

2.3. Interaction and dynamics of defects.

As stated above, radial and hyperbolic hedgehogs couple in 3D uniaxial nematic, by a *soliton string* in which most of the energy is concentrated, Fig.4. For the pair of hedgehogs of opposite topological charge, the director field within the soliton can be written as [54]

$$\mathbf{n} = \left(\frac{x}{r} \sin \theta, \frac{y}{r} \sin \theta, \cos \theta \right), \text{ where } \theta = 2 \arctan \frac{r_{\perp}}{r}, \quad r = \sqrt{x^2 + y^2}, \text{ and } r_{\perp} \text{ is the soliton}$$

radius and z -axis is the axis of rotation symmetry. In an infinite sample, from the point of

view of the Frank-Oseen model, there is no mechanism and no typical length to keep r_{\perp} from becoming a zero; when $r_{\perp} \rightarrow 0$, the energy per unit length of the string attains its minimum value $4\pi K$ [54]. As the director gradients diverge at the core for $r_{\perp} \rightarrow 0$, a more refined approach is needed. Penzenstadler and Trebin [47] considered the Landau-de Gennes theory in which the high density of director distortions is relaxed by changing the uniaxial orientational order into the biaxial one, in the spirit of Lyuksyutov's approach to the problem of the singular core of disclinations and point defects [41,46]. They demonstrated that the soliton can decay into a uniform director structure $\mathbf{n}=\text{const}$ by a mechanism of *escape to biaxiality* [47]. However, the decay might be prevented by the energy barrier separating the uniform state from the soliton state. A stabilization mechanism has been found by Semenov [54], who added a 4th-order gradient term to the standard 2nd order Frank-Oseen functional,

$f_{Fr} = \frac{K}{2}(\nabla\mathbf{n})^2 + K\xi^2(\nabla\mathbf{n})^2$. This term prescribes the soliton string to be of a (generally macroscopic) fixed radius determined by the separation distance L between the point defects located at $z = \pm L/2$ and the nematic coherence length ξ (of the order of a molecular size), namely, $r_{\perp}(z) \sim \sqrt{\xi L(1 - 4z^2/L^2)}$. The attraction force between the defects acquires a small correction term [54], $f = -4\pi K \left(1 + \frac{3}{\sqrt{2}} \frac{\xi}{L} \sqrt{\ln \frac{L}{\xi}} \right)$.

Fig.4. Schematic director configuration of the hedgehog pair connected by a soliton string.

Any realistic liquid crystal sample is bounded; the consideration above then might be applicable only when the characteristic size R of the system is much larger than L . When the two are comparable, the theory should take into account the boundary conditions, namely, the "anchoring" direction and energy associated with the director alignment at the bounding surfaces. In addition to R , the new macroscopic length scale is K/W , usually ranging $0.01 \mu\text{m}$ to $10 \mu\text{m}$. The problem becomes much more complicated and the existing models of the offer conflicting views even for the simplest geometry of a bounded sample, such as the circular capillary depicted in Fig.1. Semenov's theory [54] and the numerical analysis by Gartland et al. [55] predict that the attraction of a pair of points in the capillary can still be described by the expression above but only when L very short, much shorter than $L^* \sim d_c^{2/3} \xi^{1/3}$ that depends on the capillary diameter d_c ; for $L > d_c$, the attractive force decreases exponentially as $\exp(-6.6L/d_c)$, setting the hedgehogs "asymptotically free" and non-interactive at large separations. Qualitatively, the bounding surface sets the director field

1
2
3 practically the same on the both sides of each defect core which implies that there is no net
4 force acting on the defect. Peroli and Virga [56] also predicted an attractive potential, but of a
5 different type: the attractive force varies logarithmically with L at short distances and
6 vanishes at $L \geq 1.1d_c$. Finally, a model by Vilfan et al. [57] predicted that the defects would
7 attract only when $L < 0.1d_c$ and repel if set at a larger separations. This last model has been
8 inspired by an experimental NMR evidence that in very narrow (submicron) cylindrical
9 cavities, there might exist a (metastable) state with alternating radial and hyperbolic
10 hedgehogs separated by $L \approx d_c$ [58]; see also the numeric simulations in Ref. [59]. Although
11 all models dealt with the same basic director geometry, the boundary conditions have been
12 chosen a bit differently, which might explain the discrepancies, according to Holyst and
13 Oswald [60]: the surface anchoring was assumed to be infinitely strong, $W \rightarrow \infty$, thus rigidly
14 fixing the director orientation at the boundary in Ref. [54], but was taken finite in Ref. [57],
15 thus allowing for the (small) director deviations from the anchoring direction at the surface.
16
17

18
19 Experimentally, the interaction of the topological point defects can be studied in
20 dynamical settings, by studying whether and how the defects of opposite topological charge
21 would attract each other and annihilate. As the first example, consider two point defects in an
22 infinitely large sample, connected by a string of a constant width r whose elastic energy per
23 unit length is $\sim K$. When the two defects approach each other, the director reorientation and
24 thus energy dissipation take place mostly in the region of size $\sim r$; the drag force acting on the
25 defects moving with the closing velocity $v \sim -dL/dt$ is then $\sim \gamma_1 r v$, where γ_1 is the viscosity
26 coefficient for director reorientations. By equating this force to the elastic force $\sim K$, one
27 concludes that the two defects should approach each other with a constant velocity; or,
28 equivalently, that the distance between the defects decreases linearly with time:
29
30
31
32
33
34
35
36
37
38
39
40
41
42
43
44
45

$$L(t) \propto t_0 - t, \quad (10)$$

46
47 where t_0 denotes the moment of annihilation. Interestingly, when the soliton width tends to
48 zero, $r_{\perp} \rightarrow 0$, as in the case of infinitely large system with two point defects, then the energy
49 dissipation rate should diverge to infinity; as the elastic force remain constant, it means
50 $v \rightarrow 0$ [61]. Pismen and Rubinstein [61] interpret this result as an indication that the local
51 reduction of the uniaxial nematic order in the core region is essential for the defect interaction
52 and dynamics and deduced that the distance changes as
53
54
55
56
57
58
59
60

$$L(t) \propto \sqrt{t_0 - t}. \quad (11)$$

1
2
3
4
5
6
7
8
9
10
11
12
13
14
15
16
17
18
19
20
21
22
23
24
25
26
27
28
29
30
31
32
33
34
35
36
37
38
39
40
41
42
43
44
45
46
47
48
49
50
51
52
53
54
55
56
57
58
59
60

The dynamics obviously change when the potential of interaction changes. For example, if the interaction potential is of a logarithmic type $\sim \ln L / \xi$ (which is the case, for example, of point defects in 2D or straight parallel disclinations in 3D [62]), then the elastic force is $\sim -1/L$ and the drag force is $\sim \gamma_1 v \ln L / \xi$; therefore, the defects move with acceleration and $L(t) \propto \sqrt{t_0 - t}$, or, including the logarithmic correction, $L^2 \left(\ln \frac{L}{\xi} + const \right) \propto t_0 - t$, still similar to Eq. (11).

The dependence $L(t) \propto t_0 - t$ for the situation when the defects are indeed connected by an experimentally observable linear soliton of a constant width, over which the director experiences a rotation by 2π (similarly to Fig.4, but not axially symmetric) has been confirmed for the pairs of boojums at the surface of the hybrid aligned nematic films [21,63] and for the defects in freely suspended SmC films [64]. The stability of the soliton requires some “ordering field” [64] (e.g., an in-plane electric field [63] or a film thickness gradient [65]) to confine the director distortions within a region of a constant width. When the solitons do not exist, and the director distortions spread in the entire region between the defects, the dynamics trend changes from Eq.(10) to Eq.(11), as observed in the experimental situations [21,63,64] above and in the hybrid aligned films of thermotropic nematic polyesters with boojums [22]. Even when the solitons connecting the point exist, one can observe a crossover from $L(t) \propto t_0 - t$ to $L(t) \propto \sqrt{t_0 - t}$ when the separation distance shrinks and becomes smaller than the width of the soliton, at the late stages of annihilation [63].

The experimental situation with the point defects in circular capillaries is even more complex. Both dependencies above have been observed for annihilating pairs of hyperbolic and radial hedgehogs produced by the isotropic-to-nematic quench in circular capillaries with $d_c = 350 \mu m$ [19]: $L(t) \propto t_0 - t$ for $L \geq d_c$ and $L(t) \propto \sqrt{t_0 - t}$ for $L \leq d_c$. A similar experiment [66] with $60 \mu m \leq d_c \leq 150 \mu m$ performed for a similar thermotropic cyanobiphenyl nematic material produced a different result: The sufficiently separated pairs $L \geq d_c$ of hyperbolic and radial hedgehogs at the axis of the capillary did not show any signs of interaction; their separation remained fixed for many hours. Once set in motion by an external perturbation such as temperature gradient along the cylinder, the defects approach each other, first with $L(t) \propto t_0 - t$ when $L \geq d_c$ and with $L(t)$ exponentially vanishing at the final stages of annihilation [66]. This is in contrast to the experiment [19] where the

1
2
3
4
5
6
7
8
9
10
11
12
13
14
15
16
17
18
19
20
21
22
23
24
25
26
27
28
29
30
31
32
33
34
35
36
37
38
39
40
41
42
43
44
45
46
47
48
49
50

hedgehogs were observed to approach each other even when separated by $L \approx 6d_c$, with a constant velocity, Eq.(10), which was interpreted as the result of an elastic interaction with a constant force $\sim K$. On the other hand, the experimental technique used by Pargellis et al [19] to produce the defects, namely a fast temperature or pressure quench, might have led to temperature gradients capable of setting the hedgehogs into motion even in the absence of such an interaction. For example, the temperature difference on the two sides of a hedgehog would cause a difference in the Frank elastic constants and thus in the elastic energies of these two regions. Hilling and Saupe, see Ref. [67], also find $L(t) \propto t_0 - t$ for $L \geq d_c$. However, Ref. [67] interprets it as the result of the imperfection in the normal alignment at the cylindrical wall rather as the result of any proper elastic interaction between the defects which was taken as non-existent for $L \geq d_c$. To illustrate the point, consider Fig.1 and assume that the director at the boundary slightly deviates from the perpendicular orientation, by an angle φ , say, downwards, so that the director ticks at the right boundary in Fig.1 turn from 3 o'clock towards 4 o'clock and the ticks at the left boundary turn from 9 o'clock towards 8 o'clock. Such a deviation might quite naturally be induced by the flow of the nematic fluid during the capillary filling. Then the elastic energy (per unit length) of the configuration that escapes "downwards" (between the two defect cores in Fig.1) will be larger than the energy and "upward" escape (outside the defect pair), as the director rotate by $\pi + 2\varphi$ across the capillary in the first case and by $\pi - 2\varphi$ in the second case. The energy of the escaped configuration scales as $\sim K$ (it is independent of d_c [4]) and so does the difference in the elastic energies (per unit length) of the two regions. Therefore, the defects would approach each other to reduce the length of the "overdistorted" region and the dynamics should follow Eq.(10) [67]. By reversing the sign of φ , the same argument should see the two defects in Fig.1 moving in opposite direction: the two would repel each other rather than attract [67]. It might be of interest to verify this feature in experiments by establishing the polarity of the director tilt with respect to the polarity of the hedgehog pair(s).

51
52
53
54
55
56
57
58
59
60

To conclude, the only relatively well established experimental result for a pair of hedgehogs in circular capillaries is that at short distances, $L \leq d_c$, their dynamics can be described by Eq.(11) (as also confirmed in numerical simulations with the Lebwohl-Lasher lattice model [68]). What happens at $L \geq d_c$ is not entirely clear. Recently, Holyst and Oswald [60] proposed to use a somewhat different geometry, a set of hedgehogs at the singular disclination line that forms near a cylindrical meniscus of a nematic sample in

1
2
3 contact with air. Subsequent experiments left the group “certain that “+1” and “-1” defects
4 attract each other over at short distances and repel at large distances” [69]. Note that all the
5 experiments performed so far reduced to the passive observations of defects locations and
6 their change in time; in the future, it might be useful to add a new experimental technique of a
7 controlled trapping and manipulating the defects with optical tweezers, see, e.g., [70,71].
8
9

10
11 An important feature of the hedgehog dynamics at short separation distances
12 established by Cladis and Brandt [66] is that the radial and hyperbolic hedgehogs move
13 towards each other in the capillary with different velocities, the former moving noticeably
14 faster than the second one, especially near the nematic-to-smectic transition, where the bend
15 deformations characteristic for the hyperbolic defect become accompanied by a very large
16 elastic constant. The result is most probably related to the backflow effect, i.e. the flow of the
17 nematic fluid caused by director reorientation. Although the backflow effect is of certain
18 importance in any defect dynamics problem, it is extremely difficult to incorporate into the
19 models and is usually neglected. Nevertheless, Blanc et al. [72] recently demonstrated that in
20 the similar problem of dynamics of two linear disclinations, the difference in the velocities of
21 the defects of different strength is related to the backflow effect rather than to the elastic
22 anisotropy.
23
24
25
26
27
28
29
30
31
32

33 The dynamics of defects has been attracted interest also from the point of view of the
34 phase transitions scenarios, not only in liquid crystals and condensed matter, but also in
35 cosmological models (the Kibble model and Zureck model, for example [73]). During the
36 quench from the highly symmetric phase (such as the isotropic fluid) to the lower symmetry
37 phase (a uniaxial nematic, for example), the different pieces of the new phase might acquire
38 different values of the order parameter phase (the director orientation) [4]; when they expand
39 and meet each other, these differences produce topological defects. The quench is then
40 followed by a relaxation process in which the density N of defects decreases as the result of
41 their annihilation; for the hedgehogs, the rule should be $N(t) \propto L^{-D}$, in D -dimensional space,
42 see, e.g., [74,75]. The isotropic-to-nematic transition has attracted especial interest in this
43 regard [15,76], mostly because of the (apparent) ease with which the experimental data can be
44 created and collected. The latest theoretical result predicts that in 3D, the hedgehog densities
45 should decay as $N(t) \propto L^{-3} \propto t^{-3/2}$ if there are no other defects such as disclinations. In the
46 experiments by Chuang et al. [15], however, the number of hedgehogs has been observed first
47 to increase immediately after the quench, then reach a maximum and quickly decrease,
48 approximately as $N(t) \propto t^{-3}$. These unusual features might be related to the presence of
49
50
51
52
53
54
55
56
57
58
59
60

disclinations and to the mutual transformations of hedgehogs and disclination rings. A direct hedgehog-hedgehog annihilation in the 3D nematic bulk without disclination lines involved has been reported to obey Eq.(11) [77]. The same behaviour (11) with $N(t) \propto L^{-2}$ has been observed by Dierking et al. [78] for the annihilation dynamics of umbilic defects in 2D. A single umbilical defect represents a pair of two surface defects-booiums on the opposite sides of the flat cell filled with the nematic of a negative dielectric anisotropy; they appear when a strong electric field is applied to the cell and the director realigns from its original homeotropic orientation. As in the case with the pair annihilation in a cylindrical capillary, much more needed to be done before the dynamics of defect tangles in quenched systems with hedgehogs and disclinations can be completely understood. Note that for the clarification of the role of backflow effect the studies of dynamics of booiums and umbilics might be very productive: the singular (molecular) core that creates problem in many computer simulations does not exist here, as the “cores” of the surface defects and umbilics are macroscopic.

3. Singular points in nematic colloidal suspensions

Colloids in which the liquid crystal is either a dispersed component [79] or nematic colloids in which the liquid crystal serves as a medium containing droplets of water or solid particles [80,81], are populated by point defects whenever the surface anchoring at the interfaces is strong enough ($R \gg K/W$). Different boundary conditions (director normal to the interface, tangential, or tilted) lead to two different types of point defects. For example, the equilibrium state of a spherical nematic droplet with normal orientation corresponds to a radial hedgehog (or its topological equivalent such as a ring), while tilted or tangential orientation lead to booiums (surface defects), Fig.5.

Fig. 5: Experimental textures of radial (a) and twisted bipolar nematic droplets (b) viewed between two crossed polarizers.

The topological characteristics of all point defects in a single connected nematic volume must satisfy the restrictions imposed by the Euler-Poincaré and Gauss theorems. For p hedgehogs and q booiums enclosed by a surface of an Euler characteristic E , the restrictions write [20]

$$\sum_{i=1}^{q+p} N_i = E/2; \quad \sum_{j=1}^p k_j = E . \quad (12)$$

1
2
3
4
5
6
7
8
9
10
11
12
13
14
15
16
17
18
19
20
21
22
23
24
25
26
27
28
29
30
31
32
33
34
35
36
37
38
39
40
41
42
43
44
45
46
47
48
49
50
51
52
53
54
55
56
57
58
59
60

The conservation laws given by Eqs. (12) can influence the late stages of the first-order isotropic-to-nematic phase transition that occurs through nucleation of nematic droplets. The droplets grow by adding molecules from the surrounding isotropic matrix and by coalescence. At early stages, the droplets are small and the director within them is practically uniform; they might form defects upon coalescence according to the Kibble mechanism, when three or more nematic droplets with different director orientation coalesce. However, as soon as the droplets grow above $R_c = K/W$, each of them acquires topological defects obeying Eq.(12). For the popular nematic pentylcyanobiphenyl (5CB), the surface anchoring coefficient at the nematic-isotropic interface is $W \approx 10^6$ J/m² [82] while $K \approx 2 \times 10^{12}$ J/m² [83]; therefore the anchoring-induced production of defects becomes effective for $R \geq R_c \approx 2$ μ m. Figure 6 shows nematic droplets growing from the isotropic melt (E7 mixture containing cyanobiphenyls, similar to 5CB): supramicron droplets clearly carry stable topological defects. Because of the surface anchoring that sets tilted conical director orientation (similar to 5CB, see [82]) there are both boojums and disclination loops [20]. As Fig.6 demonstrates, the anchoring mechanism is extremely effective, producing one disclination loop per each nematic "bubble" of the appropriate size. Bowick et al. [84] expanding on the earlier studies by Chuang et al. [15], have discovered that the number of "strings" (disclinations) produced in the isotropic-nematic transition is about 0.6 per nematic "bubble" (droplet). Although this number has been found to be in reasonable agreement with the Kibble mechanism [84], it might also signal a significant contribution from the anchoring mechanism, as many droplets in the experiment [84] have been larger than 10 μ m. The balance of Kibble and anchoring mechanisms in defect production during the isotropic-nematic phase transition is still an open problem. Clearly, it should strongly depend on the speed and depth of quenching; fast quench that produces numerous sub-micron nuclei separated by submicron distances might avoid the anchoring mechanism. The critical radius of nucleation is (see, for example, [4]) $\rho_c = 2\sigma/f$, where $\sigma \sim 10^{-5}$ J/m² [82] is the surface tension coefficient for the isotropic-nematic interface, and f is the bulk energy density difference between the isotropic and nematic phases. Estimating $f \sim \Delta T \Delta H / T_{IN}$, where $\Delta T = T_{IN} - T$ is the depth of temperature quench and $\Delta H \sim 10^5$ J/m³ is the latent heat of transition [85], one finds the critical radius ranging from $\rho_c \sim (0.01-0.1)$ μ m when the quench is a 1-10 degrees below T_{IN} and to $\rho_c \rightarrow \infty$ when $T \rightarrow T_{IN}$. Therefore, even a fast temperature quench might lead to large

1
2
3 droplets if it is not deep enough. On the other hand, slow quench might tell a story of
4 anchoring-induced defect dynamics in growing droplets that is of interest on its own,
5 irrespective of the Kibble mechanism.
6
7

8
9 In the nematic droplets, the equilibrium director configuration and the corresponding
10 defects change when the boundary conditions change; for example, one can cause
11 transformations between bipolar structure with a pair of boojums and a hedgehog by changing
12 the temperature of the sample which in its turn changes the surface orientation from tangential
13 to normal [20,86]. Director deformations associated with the defect structures in the droplets
14 can cause flexoelectric polarization that contributes to electrostatic interactions between the
15 nematic droplets [87,88,89].
16
17

18
19 Point defects help to stabilize the nematic emulsions [90]. For example, imagine an
20 isotropic (say, water) droplet with a normal boundary conditions (that can be set by adding a
21 small amount of a surfactant such as lecithin to the system) in the nematic sample with a
22 uniform director. If the droplet is large, then it would distort the director around itself acting
23 as a radial hedgehog with an enlarged “core”. If the far-field of the director is uniform, then
24 such a droplet would create a satellite hyperbolic hedgehog that balances the topological
25 charge $N = 1$ of the droplet. The director field around the droplet adopts a dipole
26 configuration. When there are many droplets in the system, they attract each other at large
27 distances and repel at distances comparable to the droplet diameter $2R$ and thus form chains
28 of alternating droplets and hyperbolic hedgehogs. For distances $d \gg 2R$, the elastic force of
29 attraction scales as $F \propto KR^4/d^4$ [90], which has been experimentally verified for the case of
30 ferrofluid droplets [91] and most recently for solid particles manipulated by optical tweezers
31 in the nematic bulk [71,92].
32
33

34
35 A spectacular illustration of the role of point defects and the critical size $R_c \approx K/W$
36 in stabilization of emulsions has been found by Loudet et al [93] who demonstrated that small
37 isotropic oil droplets phase separating from the nematic host E7, can grow till their radius
38 approaches $R_c \approx 2 \mu m$; after that, each oil drop forms a satellite hyperbolic hedgehog; the
39 droplets attract each other into long chains parallel to the alignment direction of the nematic
40 phase. Ultimately, a highly ordered array of parallel macroscopic chains is formed, made of
41 monodisperse droplets which do not coalesce, in sharp contrast to the scenarios of phase
42 separation in isotropic fluids. Note that the distortions around the droplets can drive them to
43 accumulate in specific regions of the nematic matrix such as other defects (disclinations) [94]
44 and interfaces [95,96].
45
46
47
48
49
50
51
52
53
54
55
56
57
58
59
60

1
2
3
4
5
6
7
8
9
10
11
12
13
14
15
16
17
18
19
20
21
22
23
24
25
26
27
28
29
30
31
32
33
34
35
36
37
38
39
40
41
42

If the role of the surface anchoring is reduced (or if the electric field is applied to the droplet [97,98]), the hyperbolic hedgehog can be transformed into an equatorial disclination loop embracing the droplet, which is known as the Saturn-ring configuration, first envisioned theoretically in [99] on the basis of Frank-Oseen theory; and then observed experimentally in thermotropic [100,101] as well as lyotropic nematics [102], Fig. 7. Computer simulations also suggest that the hyperbolic hedgehog can transform into the Saturn ring when the size of the spherical particle decreases [103,104]. The interparticle interactions acquire a quadrupole symmetry when the dipole hedgehog configuration changes to that of the Saturn ring symmetry in the external electric field, as demonstrated by Loudet and Poulin [98].

The interparticle interactions become much weaker, $F \propto 1/d^6$, when the normal boundary conditions are changed to the tangential ones [105,106]. The director field acquires two defects-boojums at the poles of the particle and the symmetry of a quadrupole. As established experimentally with the help of optical tweezers [107], the interaction might be of repulsive or attractive nature, depending on the mutual position of the two droplets, but it deviates from the quadrupolar model when the distances between the particles become comparable to a few D 's.

The studies of dynamics of defect formations in colloidal systems are at the stage of infancy [108,109]. For example, Stark and Ventzki [108] calculated the Stokes drag of spherical particles moving in a nematic host for three different configurations shown in Fig.7. The hedgehog configuration is very different from the other two because of its dipolar symmetry.

43
44
45
46
47
48
49
50
51
52
53
54
55
56
57
58
59
60

Fig. 6: The sequence of textures of nematic nuclei at the isotropic-to-nematic transition caused by temperature quench in the mixture E7 as viewed between two crossed polarizers. The nuclei carry boojums (black arrows) and disclination loops (white arrows) (a,b); merging (c) results in disclinations with ends trapped at the cell's plates. Cell thickness $200 \mu\text{m}$.

Fig. 7: A spherical inclusion in a uniformly aligned nematic matrix with homeotropic boundary conditions resembles a radial hedgehog and produces a hyperbolic satellite when its size is much larger than the anchoring extrapolation length K/W (a); causes a Saturn ring configuration when the two are comparable (b); and is being ineffective to distort the director when much smaller than K/W (c).

4. Conclusion

The large birefringence of liquid crystals allow easy optical microscopy observations of defects, whose number is scarce in the field of view, due to the viscous relaxation of the sample inhomogeneities; observed defects are usually in equilibrium with the boundary conditions, and of small energy. This explains why *topological point defects* in condensed

1
2
3 matter physics were discovered there, in parallel with the investigations on Bloch points in
4 magnetic bubbles [110]. This is at the origin of a noticeable (but limited) series of
5 observations and, above all, of theoretical developments, including the topological theory of
6 defects and their elastic and dynamic properties. The present day observation resolution is far
7 below the advances made thanks to computational methods, in particular in the structure of
8 the core and the anisotropy of the Frank coefficients; new experimental methods are thus all
9 wanting. One can however expect that more recent optical methods, such as ultra rapid
10 confocal polarizing microscopy, attended by laser manipulations of small particles (*e.g.* in
11 nematic colloidal suspensions) or even of defects themselves, might help in the investigation
12 of macroscopic dynamic properties, at least.

13
14
15
16
17
18
19
20
21 ODL acknowledges useful discussions with E. C. Gartland, Jr. and partial support
22 through NSF grants DMR-0504516 and DMS -0456221.
23
24

25
26
27
28 **REFERENCES**
29

- 30
31 [1] L. Michel, *Rev. Mod. Phys.* **52** 617 (1980).
32 [2] H. Poincaré, *J. Math.* **2** 151(1886).
33 [3] F. R. N. Nabarro, *J. Physique* **33** 1089 (1972).
34 [4] M. Kleman and O. D. Lavrentovich, *Soft Matter Physics, an Introduction* (Springer, New York, 2003).
35 [5] M. Kleman, O. D. Lavrentovich, and Y. A. Nastishin in *Dislocations in Solids* edited by F. R. N. Nabarro and
36 J. P. Hirth, **12** 150 (2005).
37 [6] D. Hilbert and S. Cohn-Vossen, *Geometry and the Imagination* (Chelsea Pub. Cy, New York, 1954).
38 [7] M. Kleman, *Philos. Mag.* **27** 1057 (1973).
39 [8] G. E. Volovik and V. P. Mineyev, *Zh. Eksp. Teor. Fiz.* **72** 2256 (1976) [*Sov. Phys. JETP (USA)* **45** 1186
40 (1977)].
41 [9] F. R. N. Nabarro, *Conference on Fundamental Aspects of the Theory of Dislocations*, Gaithersburg, April
42 1969. NBS Special Publi. **317** 593 (1970).
43 [10] D. Melzer and F. R. N. Nabarro, *Philos. Mag. a)*- **35** 901(1977); *b)*- **35** 907(1977).
44 [11] R. B. Meyer, *Mol. Cryst. Liq. Cryst.* **16** 355 (1972).
45 [12] I. Chuang, B. Yurke, A. N. Pargellis, and N. Turok, *Phys. Rev.* **E47** 3343 (1993).
46 [13] M. Hindmarsh, *Phys. Rev. Lett.* **75** 2502 (1995).
47 [14] T. W. B. Kibble, *J. Phys.* **A9** 1387 (1976).
48 [15] I. Chuang, R. Durrer, N. Turok, and B. Yurke, *Science* **251** 1336 (1991)
49 [16] C. Williams, P. Piéranski, and P. E. Cladis, *Phys. Rev. Lett.* **29** 90 (1972).
50 [17] A. Saupe, *Molec. Cryst. Liq. Cryst.* **21** 211 (1973).
51 [18] C. Williams, P. E. Cladis, and M. Kléman, *Molec. Cryst. Liquid Cryst.* **21** 355 (1973).
52
53
54
55
56
57
58
59
60

- 1
2
3
4
5 [19] A. Pargellis, N. Turok, and B. Yurke, Phys. Rev. Lett. **67** 1570 (1991).
6 [20] G. E. Volovik and O. D. Lavrentovich, Zh. Eksp. Teor. Fiz. **85** 1997 (1983) [Sov. Phys. JETP (USA) **58**
7 1159 (1983)].
8 [21] O. D. Lavrentovich and S. S. Rozhov, Pis'ma Zh. Eksp. Teor. Fiz. **47** 210 (1988) [Sov. Phys. JETP Lett., **47**
9 254 (1988)].
10 [22] D.-K. Ding and E. L. Thomas, Mol. Cryst. Liq. Cryst. **241** 103 (1994).
11 [23] R. B. Meyer, Philos. Mag. **27** 405 (1973).
12 [24] P. E. Cladis and M. Kleman, J. Physique **33** 591 (1972).
13 [25] S. I. Anisimov and I. Dzyaloshinskii, Sov. Phys. JETP **36** 774 (1972).
14 [26] G. Mazelet and M. Kleman, Polymer **27** 714 (1986).
15 [27] C. Chiccoli, I. Feruli, O. D. Lavrentovich, P. Pasini, S. V. Shiyonovskii, and C. Zannoni, Phys. Rev. **E66**
16 030701(R) (2002).
17 [28] S. Candau, P. Le Roy and Debeauvais, Mol. Cryst. Liq. Cryst. **23** 283 (1973).
18 [29] L.A. Madsen, T.J. Dingemans, M. Nakata, and E.T. Samulski, Phys. Rev. Lett. **92** 145505 (2004)
19 [30] B.R. Acharya, A. Primak, and S. Kumar, Phys. Rev. Lett. **92** 145506 (2004).
20 [31] G. E. Volovik, Sov. Phys. JETP Lett. **28**, 59 (1978).
21 [32] M. J. Press and A. S. Arrott, J. Physique **36** C1-177 (1975)
22 [33] H. Brezis, J.-M. Coron, and E. H. Lieb, Comm. Math. Phys. **107** 647 (1986).
23 [34] S. Ostlund, Phys. Rev. **B24** 485 (1981).
24 [35] W. F. Brinkman and P. E. Cladis, Physics Today **35** 48 (1982).
25 [36] M. J. Press and A. S. Arrott, Phys. Rev. Lett. **33** 403 (1974).
26 [37] O. D. Lavrentovich and V. V. Sergan, Nuovo Cimento, Ser. D – Cond. Matt. **12** 1219 (1990).
27 [38] R.D. Williams, J. Phys. A **19** 3211 (1984);
28 [39] P. Prinsen and P. van der Schoot, J. Phys.: Condens. Matter **16** 8835 (2004)
29 [40] F. Hélein, C. R. Acad. Sci. Paris **305** 565 (1987).
30 [41] I. F. Lyuksyutov, Zh. Eksp. Teor. Fiz. **75** 358 [Sov. Phys. JETP **48** 178 (1978)].
31 [42] H. Mori and H. Nakanishi, J. Phys. Soc. Japan **57** 1281 (1988).
32 [43] O. D. Lavrentovich, T. Ishikawa, and E. M. Terentjev, Mol. Cryst. Liq. Cryst. **299** 301 (1997).
33 [44] V.G. Bodnar, O.D. Lavrentovich, V.M. Pergamenschik, Zh. Eksp. Teor. Fiz. **101**, 111 (1991) [Sov. Phys.
34 JETP **74**, 60 (1992)]
35 [45] J.-i. Fukuda and H. Yokoyama, Phys. Rev. **E66** 012703 (2002).
36 [46] N. Schopol and T. J. Sluckin, J. Physique (France) **49** 1097 (1981).
37 [47] E. Penzenstadtler and H.-R. Trebin, J. Physique (France) **50** 1027 (1981).
38 [48] R. Rosso and E. G. Virga, J. Phys. A: Math. Gen. **29** 4247 (1996).
39 [49] N. Schopol and T. J. Sluckin, Phys. Rev. Lett. **59** 2582 (1987).
40 [50] P. Biscari, G. Guidone Peroli, and T. J. Sluckin, Mol. Cryst. Liq. Cryst. **292** 91 (1997).
41 [51] E. C. Gartland, Jr. and S. Mkaddem, Phys. Rev. **E59** 563 (1999); S. Mkaddem and E. C. Gartland, Jr., Phys.
42 Rev. **E62**, 6694 (2000).
43 [52] a)-S. Kralj, E. G. Virga, and S. Zumer, Phys. Rev. **E60** 1858 (1999); b)-S. Kralj and E. G. Virga, J. Phys.
44 A: Math. Gen. **34** 829 (2001).
45
46
47
48
49
50
51
52
53
54
55
56
57
58
59
60

- 1
2
3
4
5 [53] *Defects in Liquid Crystals: Computer simulations, theory and experiment* edited by O. D. Lavrentovich, P.
6 Pasini, C. Zannoni, and S. Zumer (Kluwer Academic Publishers, the Netherlands, 2001).
7 [54] A. N. Semenov, Europhys. Lett. **46** 631 (1999)
8 [55] E.C. Gartland, Jr., A.M. Sonnet, E.G. Virga, Continuum Mech. Thermodyn. **14**, 307 (2002)
9 [56] G. Guidone Peroli and E. G. Virga, Phys. Rev. **E54** 5235 (1996); **56**, 1819 (1997).
10 [57] I. Vilfan, M. Vilfan, and S. Zumer, Phys. Rev. **A43** 6875 (1991)
11 [58] G.P. Crawford, M. Vilfan, J.W. Doane, I. Vilfan, Phys. Rev. **A 34**, 835 (1991)
12 [59] Z. Bradac, S. Kralj, S. Zumer, Phys. Rev. E **58**, 7447 (1998)
13 [60] R. Holyst and P. Oswald, Phys. Rev. **E65** 041711 (2002).
14 [61] L. M. Pismen and B. Y. Rubinstein, Phys. Rev. Lett. **69** 96 (1992).
15 [62] Y.A. Dreizen, A.M. Dykhne, Sov. Phys. JETP **34**, 1140 (1972).
16 [63] K. Minoura, Y. Kimura, K. Ito, R. Hayakawa, and T. Miura, Phys. Rev. **E 58**, 643 (1998).
17 [64] A.N. Pargelis, P. Finn, J.W. Goodby, P. Panizza, B. Yurke and P.E. Cladis, Phys. Rev. A **46**, 7765 (1992)
18 [65] D.R. Link, M. Nakata, K. Ishikawa, H. Takezoe, Phys. Rev. Lett. **87**, 195507 (2001)
19 [66] P. E. Cladis and H. R. Brand, Physica A **326** 322 (2003).
20 [67] G. G. Peroli, G. Hilling, A. Saupe, and E.G. Virga, Phys. Rev. E **58**, 3259 (1998)
21 [68] M. Svetec, Z. Bradac, S. Kralj, and S. Zumer, Mol. Cryst. Liq. Cryst. **413**, 43 (2004)]
22 [69] A. Zywockinski, K. Pawlak, R. Holyst, P. Oswald, J. Phys. Chem. B **109**, 9712 (2005).
23 [70] J.-I. Hotta, K. Sasaki, H. Masuhara, Appl. Phys. Lett. **71**, 2085 (1997)
24 [71] I.I. Smalyukh, A.N. Kuzmin, A.V. Kachynski, P.N. Prasad, and O.D. Lavrentovich, Appl. Phys. Lett. **86**
25 021913 (2005).
26 [72] C. Blanc, D. Svensek, S. Zumer, and M. Nobili, Phys. Rev. Lett. **95**, 097802 (2005).
27 ⁷³ *Patterns of Symmetry Breaking* edited by H. Arodz, J. Dziarmaga and W.H. Zurek (Kluwer Academic
28 Publishers, the Netherlands, 2003).
29 [74] H. Toyoki, Phys. Rev. **A 42**, 911 (1990).
30 [75] R.A. Wickham, Phys. Rev. E **56**, 6843 (1997)
31 [76] M. J. Bowick, L. Chandar, E. A. Schiff and A. M. Srivastava, Science **263** 943 (1994).
32 [77] A.N. Pargellis, J. Mendez, M. Srinivasarao, B. Yurke, Phys. Rev. E **53**, R25 (1996).
33 [78] I. Dierking, O. Marshall, J. Wright, and N. Bulleid, Phys. Rev. E **71**, 061709 (2005).
34 [79] P.S. Drzaic, *Liquid Crystal Dispersion* (World Scientific, Singapore, 1995).
35 [80] H. Stark, Physics Reports **351**, 387 (2001).
36 [81] P. Poulin, Curr. Opin. Colloid & Interf. Sci. **4**, 66 (1999).
37 [82] S. Faetti, V. Palleschi, Phys. Rev. **A 30**, 3241 (1984).
38 [83] M.J. Bradshaw, E.P. Raynes, J.D. Bunning, T.E. Faber, J. Physique **46**, 1513 (1985).
39 [84] M.J. Bowick, L. Chandar, E.A. Schiff, A.M. Srivastava, Science **263**, 943 (1994).
40 [85] H. Yokoyama, J. Chem. Soc. Faraday Trans. **2**, 84 (1988).
41 [86] O.O. Prishchepa, A.V. Shabanov, V. Y. Zyryanov, Phys. Rev. E **72**, 031712 (2005).
42 [87] R.B. Meyer, Phys. Rev. Lett. **22** 918 (1969).
43 [88] O.D. Lavrentovich, Pis'ma Zh. Tekh. Fiz. **14**, 166 (1988) /Sov.Tech.Phys.Lett. **14** 73 (1988).
44 [89] N.M. Golovataya, M.V. Kurik, and O.D. Lavrentovich, Liq. Cryst. **7**, 287 (1990).
45
46
47
48
49
50
51
52
53
54
55
56
57
58
59
60

- 1
2
3
4
5 [90] P. Poulin, H. Stark, T.C. Lubensky, and D.A. Weitz, *Science* **275**, 1770 (1997); T.C. Lubensky, D. Pettey,
6 N. Currier, H. Stark, *Phys. Rev. E* **57**, 610 (1998); P. Poulin, D.A. Weitz, *Phys. Rev. E* **57**, 626 (1998).
7 [91] P. Poulin, V. Cabuil, and D.A. Weitz, *Phys. Rev. Lett.* **79**, 4862 (1997).
8 [92] M. Yada, J. Yamamoto, H. Yokohama, *Phys. Rev. Lett.* **92**, 185501 (2004)
9 [93] J.-C. Loudet, P. Barois, and P. Poulin, *Nature* **407**, 611 (2000).
10 [94] D. Voloschenko, O.P. Pishnyak, S.V. Shiyonovskii, O.D. Lavrentovich, *Phys. Rev. E* **65**, 060701 (R) (2002)
11 [95] J.L. West, K. Zhang, A.V. Glushchenko, Y. Reznikov, D. Andrienko, *Mol. Cryst. Liq. Cryst.* **422**, 73 (2004)
12 [96] M. Mitov, F. De Guerville, C. Bourgerette, *Mol. Cryst. Liq. Cryst.* **435**, 673 (2004)
13 [97] H. Stark, *Eur. Phys. J. B* **10**, 311 (1999) ; *Phys. Rev. E* **66**, 032701 (2002).
14 [98] J.C. Loudet, P. Poulin, *Phys. Rev. Lett.* **87**, 165503 (2001)
15 [99] O.V. Kuksenok, R.W. Ruhwandl, S.V. Shiyonovskii, E.M. Terentjev, *Phys. Rev. E* **54**, 5198 (1996); S.V.
16 Shiyonovskii and O.V. Kuksenok, *Mol. Cryst. Liq. Cryst. A* **321**, 489 (1998).
17 [100] Y. Gu and N.L. Abbott, *Phys. Rev. Lett.* **85**, 4719 (2000).
18 [101] J.C. Loudet, O. Mondain-Monval, P. Poulin, *Eur. Phys. J.* **E7**, 205 (2002).
19 [102] O. Mondain-Monval, J.C. Dedieu, T. Gulik-Krzywicki, P. Poulin, *Eur. Phys. J.* **B12**, 167 (1999)
20 [103] A.-i. Fukuda, M.; Yoneya, H. Yokoyama, *Phys. Rev. E* **65**, 041709 (2002).
21 [104] D. Andrienko, G. Germano, M.P. Allen, *Phys. Rev. E* **63**, 041701 (2001).
22 [105] S. Ramaswamy, R. Nityananda, V. Raghunathan, and J. Prost, *Mol. Cryst. Liq. Cryst.* **228** 175 (1996).
23 [106] R.W. Ruhwandl and E.M. Terentjev, *Phys. Rev. E* **55** 2958 (1997).
24 [107] I.I. Smalyukh, O.D. Lavrentovich, A.N. Kuzmin, A.V. Kachynski, and P.N. Prasad, *Phys. Rev. Lett.* **95**,
25 157801 (2005).
26 [108] H. Stark and D. Ventzki, *Phys. Rev. E* **64**, 031711 (2001).
27 [109] J.-i. Fukuda, H. Stark, H. Yokoyama, *Phys. Rev. E* **72**, 021701 (2005).
28 [110] A. P. Malozemoff and J. C. Slonczewski, *Magnetic Domain Walls in Bubble Materials* (Academic Press,
29 New York, 1979).
30
31
32
33
34
35
36
37
38
39
40
41
42
43
44
45
46
47
48
49
50
51
52
53
54
55
56
57
58
59
60

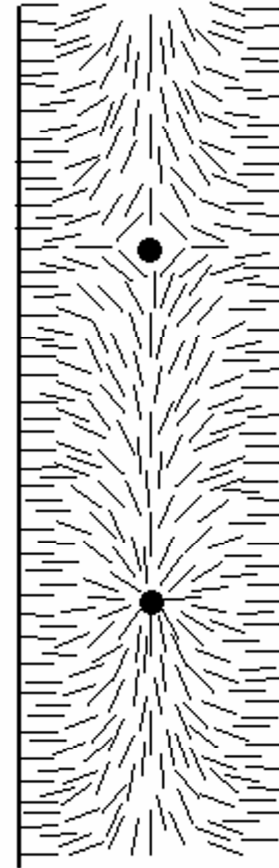


Fig.1

1
2
3
4
5
6
7
8
9
10
11
12
13
14
15
16
17
18
19
20
21
22
23
24
25
26
27
28
29
30
31
32
33
34
35
36
37
38
39
40
41
42
43
44
45
46
47
48
49

1
2
3
4
5
6
7
8
9
10
11
12
13
14
15
16
17
18
19
20
21
22
23
24
25
26
27
28
29
30
31
32
33
34
35
36
37
38
39
40
41
42
43
44
45
46
47
48
49

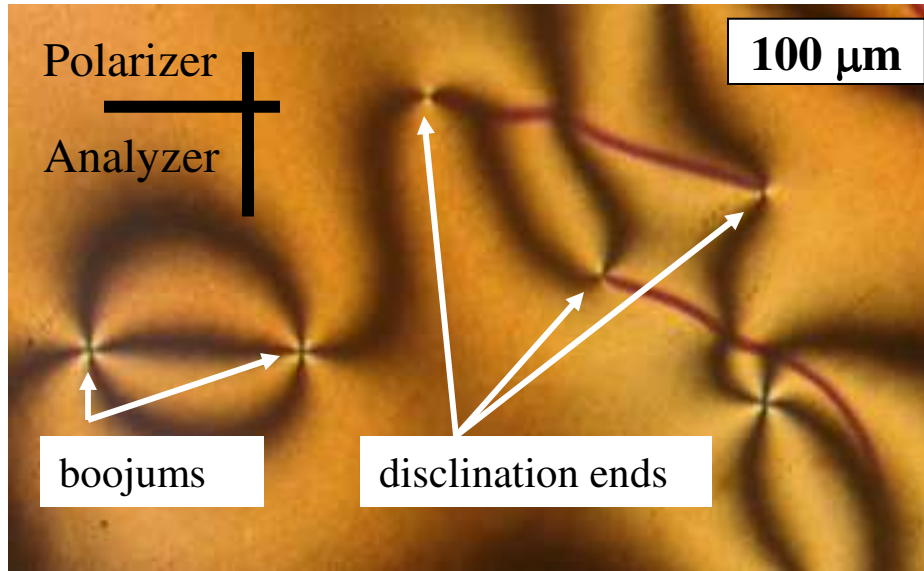


Fig.2

1
2
3
4
5
6
7
8
9
10
11
12
13
14
15
16
17
18
19
20
21
22
23
24
25
26
27
28
29
30
31
32
33
34
35
36
37
38
39
40
41
42
43
44
45
46
47
48
49

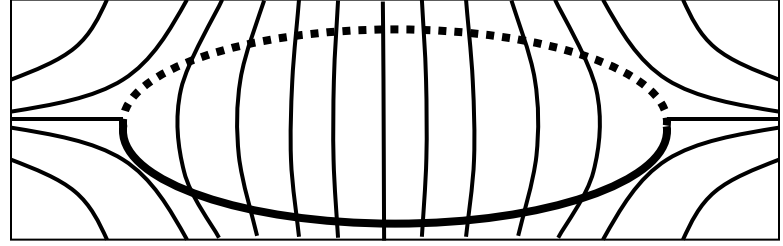
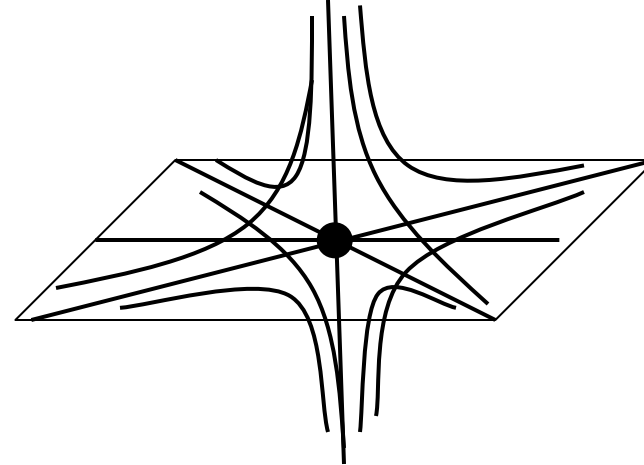
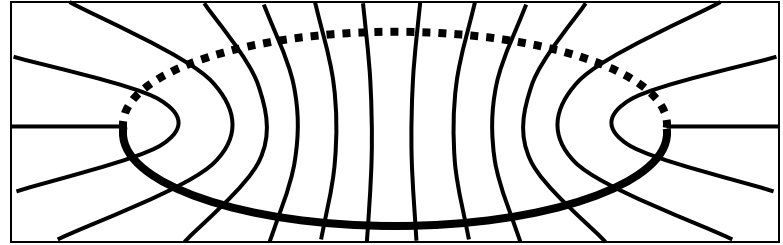
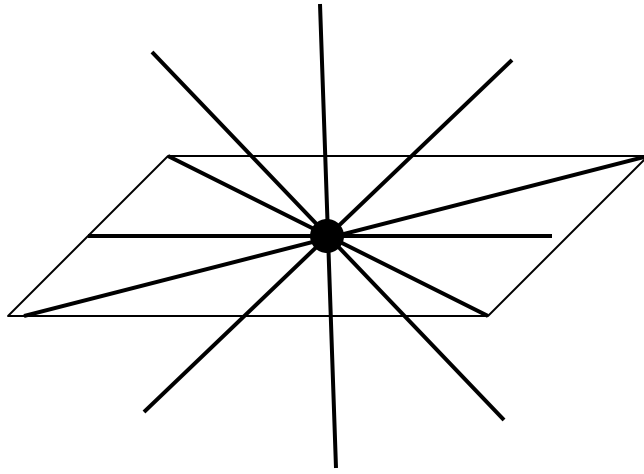


Fig.3

1
2
3
4
5
6
7
8
9
10
11
12
13
14
15
16
17
18
19
20
21
22
23
24
25
26
27
28
29
30
31
32
33
34
35
36
37
38
39
40
41
42
43
44
45
46
47
48
49

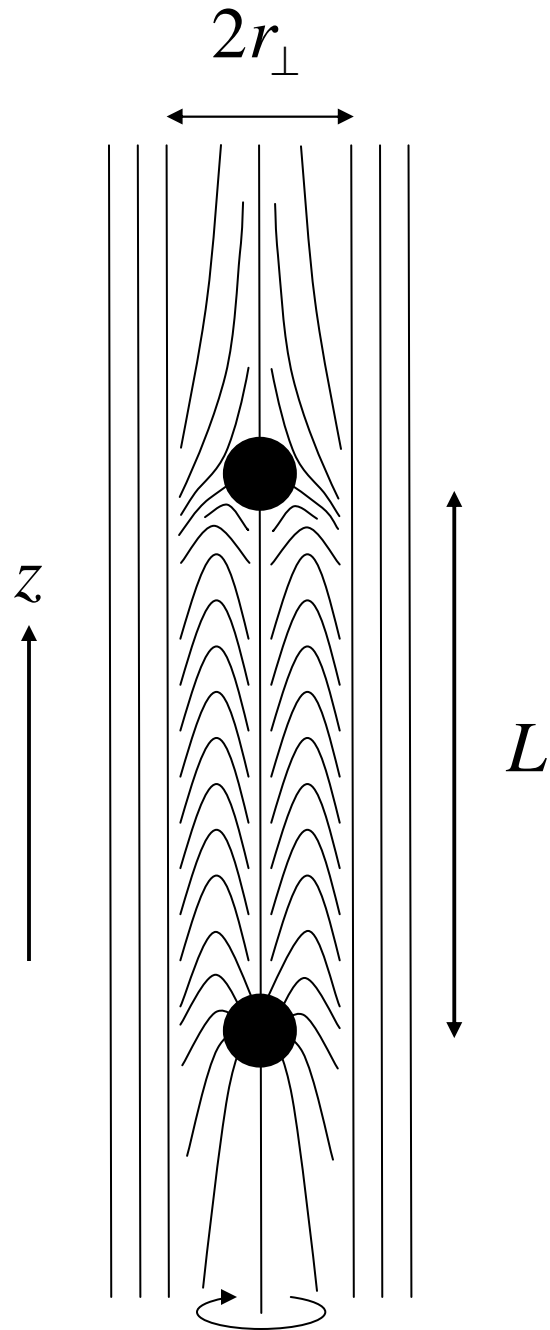


Fig.4

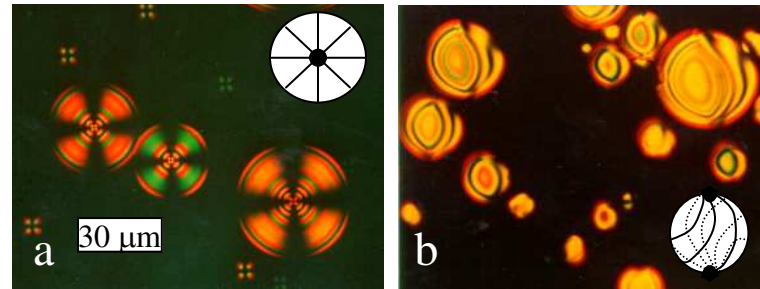
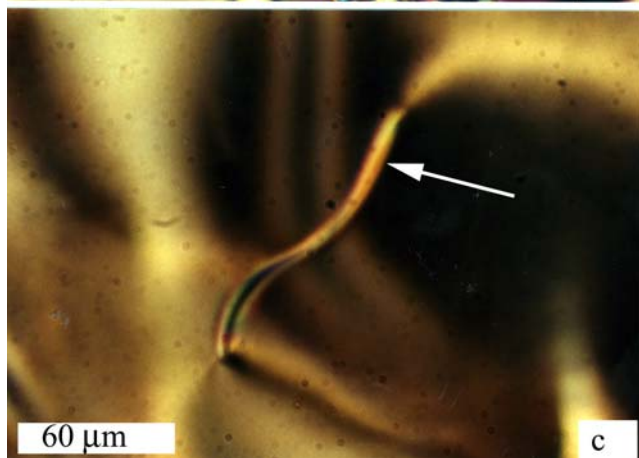
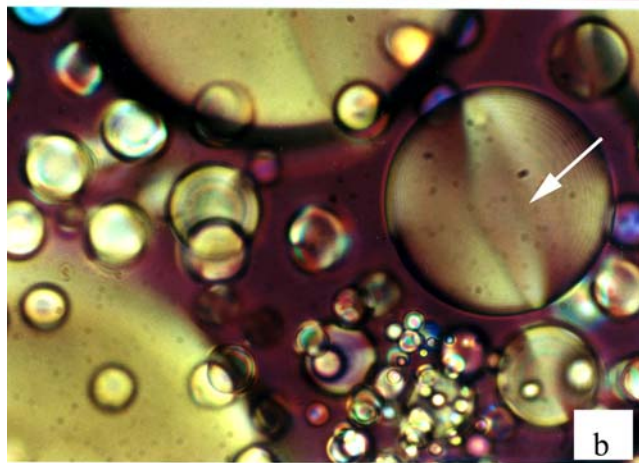
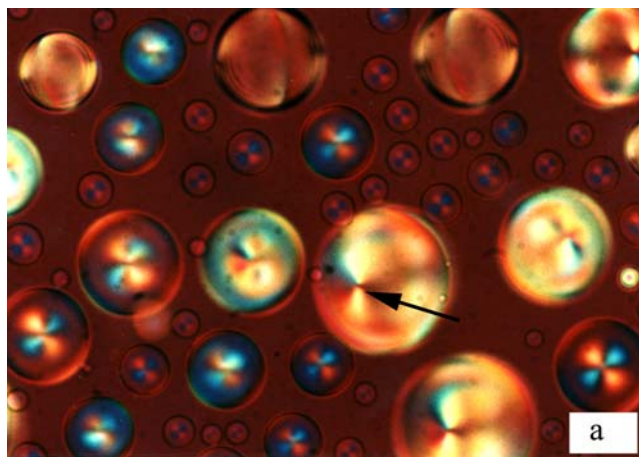


Fig.5



Pre Review Only

Fig.6

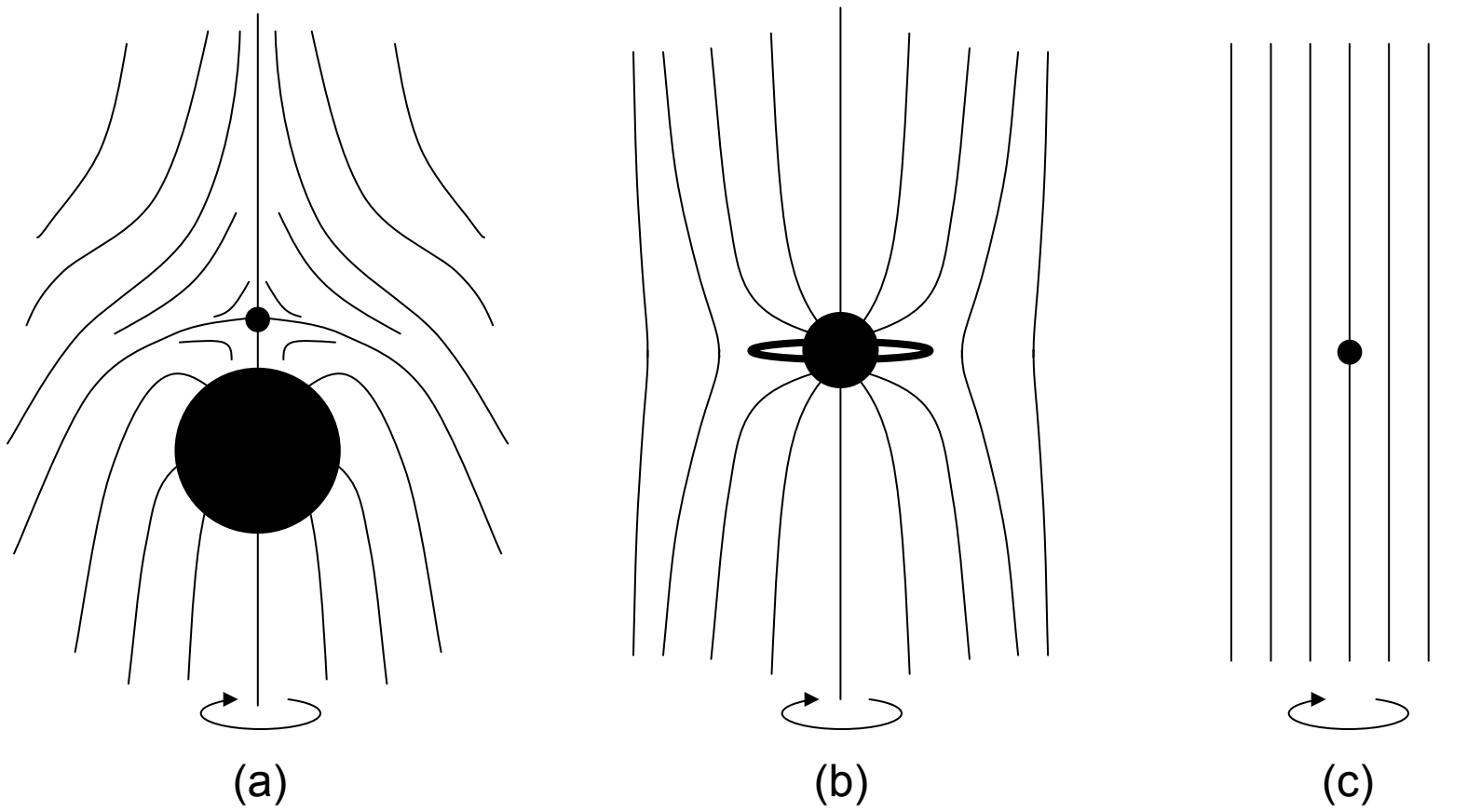


Fig. 7

1
2
3
4
5
6
7
8
9
10
11
12
13
14
15
16
17
18
19
20
21
22
23
24
25
26
27
28
29
30
31
32
33
34
35
36
37
38
39
40
41
42
43
44
45
46
47
48
49

Topological point defects in nematic liquid crystals

MAURICE KLEMAN and OLEG D. LAVRENTOVICH

Fig. 1. Capillary tube with homeotropic (*i.e.* normal) boundary conditions, meridian section. The director is in the meridian plane. Point defects $N = +1$ (radial hedgehog) and $N = -1$ (hyperbolic hedgehog).

Fig. 2. Schlieren texture in a sample with degenerate planar anchoring conditions. The sample is observed between crossed polars. There are two black brushes associated with the $k = \pm 1/2$ lines, and four brushes (the Maltese cross) associated with the $k = \pm 1$ lines.

Fig. 3. Splitting of point defects into disclination loops: a)- $N = 1 \equiv k = 1/2$; b)- $N = -1 \equiv k = -1/2$

Fig.4. Schematic director configuration of the hedgehog pair connected by a soliton string.

Fig. 5: Experimental textures of radial (a) and twisted bipolar nematic droplets (b) viewed between two crossed polarizers.

Fig. 6: The sequence of textures of nematic nuclei at the isotropic-to-nematic transition caused by temperature quench in the mixture E7 as viewed between two crossed polarizers. The nuclei carry boojums (black arrows) and disclination loops (white arrows) (a,b); merging (c) results in disclinations with ends trapped at the cell's plates. Cell thickness $200 \mu m$.

Fig. 7: A spherical inclusion in a uniformly aligned nematic matrix with homeotropic boundary conditions resembles a radial hedgehog and produces a hyperbolic satellite when its size is much larger than the anchoring extrapolation length K/W (a); causes a Saturn ring configuration when the two are comparable (b); and is being ineffective to distort the director when much smaller than K/W (c).

Topological point defects in nematic liquid crystals

MAURICE KLEMAN^{*‡} and OLEG D. LAVRENTOVICH[†]

[‡]Institut de Minéralogie et de Physique des Milieux Condensés (CNRS UMR 7590),

Université Pierre-et-Marie-Curie, Campus Boucicaut, 140 rue de Lourmel, 75015 Paris, France

[†]Chemical Physics Interdisciplinary Program and Liquid Crystal Institute, Kent State University,

Kent, Ohio 44242, USA

Abstract

Point defects in nematics, also called hedgehogs, are topological entities that have no equivalent in ordered atomic solids, despite the homonymy. They have been the subject of intense experimental and, above all, theoretical (analytic and computational) investigations in the last thirty years. They are present in bulk specimens and at the specimen boundaries. This review article stresses the importance of the core structure of the defect, of its possible splitting into a disclination loop, of the boundary conditions, and takes stock of the recent advances on point defects in nematic colloidal suspensions. An important topic is the formation of strings between opposite hedgehogs (radial and hyperbolic), and their role in the dynamic properties of nematics.

Keywords: liquid crystals, point defects, hedgehogs, boojums, topological defects

1. Introduction

A nematic liquid crystal is an anisotropic fluid formed by rod-like or disk-like molecules that tend to be parallel to a common direction, the *director*, noted \mathbf{n} ($n^2=1$). The directions \mathbf{n} and $-\mathbf{n}$ are physically equivalent: $\mathbf{n} \equiv -\mathbf{n}$. There is no long-range translational order in the system and thus nematics are fluid and very sensitive to the external field, which explains why they became a key technological material in applications such as informational displays. Nematic liquid crystals are in the focus of intensive interdisciplinary studies also because they represent a well-defined soft matter system with a rich variety of supramolecular structures, most notably those corresponding to the so-called topological defects. A topological defect is a configuration of the order parameter that cannot be transformed continuously into a uniform

1
2
3 state. They can occur during the symmetry breaking phase transitions, under an external
4 field, or simply be a necessary element of an equilibrium state. For example, in a sufficiently
5 large spherical nematic droplet with perpendicular alignment of molecules at the surface, the
6 director field forms a radial-like configuration with a point defect at the centre, in order to
7 reach an equilibrium state. This point defect in the director configuration is of a completely
8 different nature as compared to point defects such as vacancies and interstitials in solid
9 crystals [1]; its topological nature means that the distortions of the order parameter around the
10 “point” extend throughout the entire system.
11

12
13
14
15
16
17 The singular points of a *vector field* (cols, nœuds, foyers, etc) were classified by
18 Poincaré [2], by using the tools of the theory of ordinary differential equations; Nabarro[3]
19 was the first to notice that Poincaré’s method can be applied, with the purpose of classifying
20 point defects, to spins in a ferromagnet and directors in a nematic insofar as the sample does
21 not show circuits along which \mathbf{n} is reversed.
22
23
24
25

26
27 The *topological classification* of defects, on the other hand, relies on the topological
28 properties of the *order parameter space*. It does not give a classification as detailed as the
29 vector field one, but its principles can be extended to any ordered medium and to defects of
30 any dimensionality [4,5]. The scalar order parameter $S(T)$ of a uniaxial nematic is the
31 thermal mean $\frac{1}{2} \langle (3\cos^2\theta - 1) \rangle$ of the orientation of the molecules about the director. More
32 precisely, the order parameter (o.p.) is a traceless tensor $Q_{ij} = S(T)(n_i n_j - \frac{1}{3}\delta_{ij})$. The o.p.
33 space is the space of all the realizations of the o.p.. In the case of a uniaxial nematic, a sphere
34 of unit radius represents adequately all the directions of \mathbf{n} ; the o.p. space is therefore a *half*
35 sphere, namely the *projective plane*, noted P_2 , see [6]. Topological defects of various
36 dimensionalities d in ordered media are classified by the homotopy groups $\Pi_n(V)$, $n = D - d -$
37 1, where D is the space dimension; in a 3D nematic, $V = P_2$, $n = 1$ stands for line defects
38 (disclinations), $n = 2$ for point defects. The topological charge (an invariant) carried by a
39 point defect can be calculated by the relation [7]
40
41
42
43
44
45
46
47
48
49
50

$$4\pi N = \iint \varepsilon_{ijk} \varepsilon_{pqk} n_q \cdot j n_{r,k} n_p dS_i \quad (1)$$

51
52 where the integration is performed on a sphere-like surface surrounding the singular point. N
53 is an integer; $\Pi_2(V) = Z$. Point defects $N = \pm 1$, the only ones ever observed experimentally,
54 are called *hedgehogs*. Because Eq. 1 is odd in the director components and $\mathbf{n} = -\mathbf{n}$, the same
55 point defect can be assigned opposite charges: also, the charge can be drawn opposite by a
56 circumnavigation of the point defect around a disclination line of strength $k = \pm \frac{1}{2}$ (about
57
58
59
60

which the director changes sign) [8]. It is usual to assign the value $N=+1$ to a radial hedgehog, $N=-1$ to a hyperbolic hedgehog, see Fig. 1. Nabarro has probably been the first to show a keen interest in the topology of defects in a nematic [9] by noticing that the Euler-Poincaré characteristic of a sphere [5] measures the total strength of the disclinations piercing the boundary of a nematic droplet, if the boundary conditions are such that the director is everywhere parallel to the droplet surface ($\sum_i k_i = 2$).

Fig. 1. Capillary tube with homeotropic (*i.e.* normal) boundary conditions, meridian section. The director is in the meridian plane. Point defects $N = +1$ (radial hedgehog) and $N = -1$ (hyperbolic hedgehog).

The free energy density associated with the changes of the tensor order parameter in the vicinity of the nematic-isotropic phase transition is of the Landau-De Gennes form:

$$f_{LDG} = \frac{1}{2}a(T,p)\text{tr}Q^2 - \frac{1}{3}b\text{tr}Q^3 + \frac{1}{4}c(\text{tr}Q^2)^2 \quad (2)$$

When the scalar order parameter does not change much, which is true for director deformations over the scales much larger than the molecular size, then the free energy density of the elastic director distortion is written as the Frank-Oseen expression

$$f_{Fr} = \frac{1}{2}K_1(\text{div}\mathbf{n})^2 + \frac{1}{2}K_2(\mathbf{n}\cdot\text{curl}\mathbf{n})^2 + \frac{1}{2}K_3(\mathbf{n}\times\text{curl}\mathbf{n})^2 - K_{24}\text{div}(\mathbf{n}\text{div}\mathbf{n} + \mathbf{n}\times\text{curl}\mathbf{n}) \quad (3)$$

with Frank elastic constants of splay (K_1), twist (K_2), bend (K_3), and saddle-splay (K_{24}).

Nabarro made also very early observations of hedgehogs in capillaries [10]. In fact, there have been very few detailed experimental investigations of hedgehogs in the course of time since their appearance in the realm of nematics, compared to the flourishing of theoretical studies, these latter encouraged by the development of computer methods. On the other hand, theory and experiment seem to go hand in hand for point defects in colloidal suspensions in nematics, where an air bubble (which acts as a positive $N=+1$ point defect) or a droplet or a particle that compensate a negative $N = -1$ point defect in their vicinity [11], can form a stable dipole.

This paper presents a brief review of bulk point defects (hedgehogs) and surface singular points, often called boojums (the name is due to Lewis Carroll and has been adopted frenetically by the superfluid and liquid crystal communities thanks to Mermin).

2. Bulk and surface singular points.

2. 1. Static observations

1
2
3 Defects usually appear in the bulk of a sample by symmetry breaking, at the
4 isotropic→nematic transition T_{IN} , either by a thermal quench or a slow transition; pressure
5 quench has also been employed. One expects to get this way a random array of defects of
6 various dimensionalities: point defects, disclination lines, and configurations or solitons (non-
7 singular topological defects) [4]. The final defect distribution depends on the time of
8 annealing and on the boundary conditions, *i.e.* on the *anchoring* conditions at the boundaries
9 of the sample, like those induced by a physical or chemical surface treatment; this forces the
10 orientation of the molecule.
11
12
13
14
15
16

17 We are interested in *point defects*. A remarkable experimental result is that their
18 occurrence *in the bulk* just after quench (independently of the boundary conditions) is a rather
19 rare, if ever observed, event [12]. It has been given of this phenomenon an interesting (and
20 subtle) explanation [13]. The topological charge N (Eq. 1) measures twice the number of
21 times that P_2 is covered by the order parameter (the director); this is a rather difficult
22 geometric requirement to be obeyed by the correlated nematic domains which appear
23 randomly about some point of the sample at the transition. The probability of this event can
24 be calculated [13]. The idea follows the lines of the celebrated Kibble mechanism for the
25 generation of cosmic strings (considered as singularity lines) in the early universe [14], which
26 has inspired laboratory experiments on liquid crystals, see *e.g.* [15].
27
28
29
30
31
32
33
34
35

36 Hedgehogs are thus observed in special geometries with specific anchoring conditions,
37 namely in *capillaries* [10,16,17,18,19], in nematic *droplets* [20], and in confined parallel
38 samples with *hybrid boundary conditions* [21,22]. Our references are not exhaustive. On the
39 other hand, hedgehogs are the rule rather than the exception, in nematic colloidal suspensions
40 (see next section), but this also proceeds from the special anchoring conditions met in such
41 systems.
42
43
44
45

46 In capillaries with homeotropic anchoring, the molecules normal to the boundaries
47 force a radial geometry, as pictured in Fig. 1; one observes that the director ‘escapes along the
48 3rd dimension’ –namely the axis of the capillary– as nicely worded by Meyer [23]. The
49 $k = +1$ disclination forced by the boundary conditions is therefore continuous along its core
50 (or, differently stated, coreless). Observe that the escape is either up or down, with equal
51 probabilities if the normal anchoring is perfect. Thus two types of point defects do appear, of
52 opposite charges $N = \pm 1$. The director configuration can be investigated experimentally by
53 polarized light microscopy; the resulting observations satisfy the expected geometry, at least
54 qualitatively –this experimental method does not bring a large resolution. Therefore the role
55
56
57
58
59
60

played by the anisotropy of the elastic moduli K_1, K_2, K_3 in the director configuration around the hedgehogs [23,24] has not yet been satisfactorily tested.

Fig. 2. Schlieren texture in a sample with degenerate planar anchoring conditions. The sample is observed between crossed polars. There are two black brushes associated with the $k = \pm 1/2$ lines, and four brushes (the Maltese cross) associated with the $k = \pm 1$ lines.

This same anisotropy is also responsible for the configuration of the director about $k=+1$ disclination lines, but also about $k=-1$ lines; see [25]. Disclination lines can be observed end-on in well-annealed nematic samples formed between two flat glass plates (Schlieren textures, see Fig. 2). Topology requires that the sum total of the disclination charges vanishes, $\sum_i k_i = 0$. One observes $k = \pm 1/2$ and $k = \pm 1$ lines. In most experimental cases, in particular SMLCs (small molecule liquid crystals) the escaped geometry is stable with respect to planar singular $k = \pm 1$, and point defects are present; the situation is more involved in main chain PLCs (polymer liquid crystals) where usually the splay modulus is so large that the escape can be absent in a radial geometry [26]. Thus, apart a few exceptions, there is ample evidence that the integer lines are coreless and carry point defects, often located outside the sample. Monte Carlo calculations have confirmed these results [27].

The topology of a droplet with homeotropic anchoring is compatible with a radial hedgehog, but its actual presence depends on the anchoring energy $\sim W\delta^2$ (which measures the excess surface energy necessary to turn the director apart the normal direction by an angle δ , W is called the surface anchoring coefficient), and the droplet size R . Compare the surface energy, which scales as WR^2 for a uniform director, and the bulk energy, which scales as $(K/R^2)R^3 = KR$ for a radial hedgehog; it is easy to convince oneself that in a droplet of radius R smaller than approximately $R_c = K/W$ the director is uniform, whereas a larger droplet contains a radial hedgehog [4].

In a droplet with planar (degenerate) anchoring, the director field should obey the Euler-Poincaré theorem [6,9] and, accordingly, must suffer either two singularities with $k=1$ or one singularity with $k=2$. The first case (two $k=1$ singularities) is often met when a nematic droplet is suspended in an isotropic fluid such as glycerol, say [28, 20]; the second one being more specific of biaxial nematics (for the existence of which there appears to be new experimental evidences [29,30]). Note that in both cases the point defects are essentially surface defects that cannot move inside the nematic bulk because of the boundary conditions. They are thus different from the hedgehogs that can exist both in the bulk and at the surface. Because of this distinction, these surface defects are called boojums [31]; a necessary

condition for their formation is that the director field is either tangential or tilted with respect to the surface so that the defect is characterized by an invariant k in addition to N [20].

Finally, hybrid samples: a typical example is when a thin nematic film is spread onto the surface of an isotropic fluid at which the director is oriented tangentially (planar degenerate alignment) whereas the upper boundary is free. Quite often the spontaneous anchoring at the nematic-air interface is homeotropic or tilted. The competition between the two anchoring modes is relaxed by the presence of surface point defects [21,22].

2.2. Theory of the static point defect.

In the *one-constant* approximation (*i.e.* $K = K_1 = K_2 = K_3$) the geometry of a point defect can be represented near its core by the equations

$$\phi = N\theta_r + \phi_0, \quad \tan \frac{\theta}{2} = \left(\tan \frac{\lambda}{2}\right)^N \quad (4)$$

where θ , ϕ are spherical angles for the director in \mathbf{r} ; θ_r the polar angle of \mathbf{r} in the horizontal plane, λ the angle between the Oz axis and the direction \mathbf{r} [17]. It is apparent that $\theta = +\lambda$ for the star-like radial hedgehog, $\theta = -\lambda$ for the hyperbolic hedgehog. The energy does not diverge on the core; one gets, for the radial hedgehog, by integrating the free energy density all over a ball of radius R with a point defect at the centre

$$E_1 = 8\pi KR \quad (5a)$$

and

$$E_{-1} = \frac{1}{3}8\pi KR \quad (5b)$$

for the hyperbolic hedgehog [32].

Of course, there is a physical core, where the nature of the order parameter is modified with respect to the region of ‘good’ crystal. Let us write for the radial hedgehog the total energy as

$$E_1^{tot} = 8\pi K(R - r_c) + \gamma r_c^3 \quad (6)$$

Minimizing this expression, one gets

$$r_c = \sqrt{8\pi K/3\gamma}; \quad E_1^{tot} = 8\pi K\left(R - \frac{2}{3}\sqrt{8\pi K/3\gamma}\right) \quad (7)$$

r_c does not depend on the size R of the sample, and the energy is not significantly different from E_1 , if the core is microscopic compared to R , as expected. Therefore one can adopt E_1 as a first approximation for the total energy.

To find the minimizer of the integral $\frac{1}{2} \int (\nabla \mathbf{n})^2$ (one-constant approximation) in a given volume $U \subset \mathbf{R}^3$ is a problem relevant to the theory of harmonic maps with defects [33]. An interesting result is that the minimal energy $E_{U\{i\}}$ of a set $U\{i\}$ of given point defects $\{i\}$ with $N_i = \pm 1$, such that $\sum N_i = 0$, is given by the expression

$$E_{U\{i\}} = 4\pi KL \quad (8)$$

where L is the minimal total length of the dipoles formed by linking point defects of opposite signs two by two. One cannot overestimate the physical importance of this result that stresses the interactions between opposite hedgehogs. These dipoles are indeed visible in Schlieren textures. A somewhat analog result was obtained in [34,35] through a dimensional analysis, but for a unique pair.

Experimental observations show that the real situation is somewhat more complex, even if some results of the simple model above do subsist: a)- K_2 is always small compared to the other moduli; it is then expected that the radial symmetry could be broken by a twist deformation. This phenomenon has been observed for surface defects-boojuims in Schlieren textures of lens-shaped droplets [36] and for radial hedgehogs in droplets [28], and studied later for spherical bipolar droplets with pairs of boojuims at the poles, both experimentally [20,37] and theoretically [38,39]; in relation with these investigations, a radial hedgehog is *not* a minimizer in a ball with homeotropic conditions, if the Frank constants are anisotropic [40]; b) as pointed by Press and Arrott [36], the structure of defects is influenced by the splay-cancelling mechanism, according to which the energy of splay deformations along one direction can be *reduced* by splay in another direction, somewhat similar to the phenomenon of soap films adopting a catenoid shape; c)- it has been suggested by Melzer *et al.*, on the basis of their observations [10], that point defects might be split into disclination loops, of strength $k = +\frac{1}{2}$ for a radial hedgehog, of strength $k = -\frac{1}{2}$ for a hyperbolic hedgehog, Fig. 3.

Fig. 3. Splitting of point defects into disclination loops: a)- $N = 1 \Rightarrow k = 1/2$; b)- $N = -1 \Rightarrow k = -1/2$

Two *theoretical* elements have been put forward which complete the present picture of point defects in nematics a)- the divergence moduli K_{13} , K_{24} can play a role in the stability of the model, in particular might decide whether the point defect is split, or not, into a disclination loop; b)- the order parameter might change smoothly in the core region, not only in modulus, but also in character. It has indeed been suggested that it might be biaxial [41]. Computer calculations validate this suggestion. We comment on these two points.

The Frank-Oseen elastic theory in the director representation has been used in [42] and [43] to compare the energies of the hedgehogs and their disclination loop modifications. The divergence elastic term K_{24} is introduced in [43]. Eq. 5a, 5b become

$$E_{+1}^{tot} = 8\pi(K - K_{24})(R - r_c) + \gamma r_c^3 \quad (9a)$$

for a radial hedgehog, and

$$E_{-1}^{tot} = \frac{1}{3} 8\pi(K + K_{24})(R - r_c) + \gamma r_c^3 \quad (9b)$$

for a hyperbolic hedgehog. The transformation to a disclination loop of radius ρ adds in both cases a term of the order of ρK_{24} . It is clear that in the frame of this simplified model the $k = \frac{1}{2}$ loop is forced to expand if $K_{24} < 0$, to shrink if $K_{24} > 0$, the reverse being true for the $k = -\frac{1}{2}$ loop. The radius of the loop stabilizes for a value $\rho \sim \xi \exp\left(-\frac{4K_{24}}{K}\right)$, which is microscopic (ξ is the nematic coherence length). **By applying the electric field perpendicular to the loop in a nematic material with a positive dielectric anisotropy, one can expand the loop to a larger radius [44].** See [45] for a recent calculation of the hyperbolic hedgehog in the same vein, but using the full Frank moduli anisotropy.

For the study of the core itself, the Landau-de Gennes theory has been largely employed, allowing a variation of the scalar order parameter. It is shown in [46] that spherically symmetric configurations are exact solutions which minimize the Landau-de Gennes free energy, and that the core, whose size is found large compared to ξ , is isotropic. But disclination loops are also solutions. A number of papers [47,48] have exploited with success the suggestion that the core of a $|k| = \frac{1}{2}$ line is biaxial [41,49,50].

Complete models with anisotropic coefficients, divergence elastic terms, Landau expansion in the full free energy, to what has to be added the role of boundary conditions at a finite distance, produce more complicated results, see e.g. [51,52]. Of course, these new developments often require heavy computational methods, see [53].

2.3. Interaction and dynamics of defects.

As stated above, radial and hyperbolic hedgehogs couple in 3D uniaxial nematic, by a *soliton string* in which most of the energy is concentrated, Fig.4. For the pair of hedgehogs of opposite topological charge, the director field within the soliton can be written as [54]

$$\mathbf{n} = \left(\frac{x}{r} \sin \theta, \frac{y}{r} \sin \theta, \cos \theta \right), \text{ where } \theta = 2 \arctan \frac{r_{\perp}}{r}, \quad r = \sqrt{x^2 + y^2}, \text{ and } r_{\perp} \text{ is the soliton}$$

radius and z -axis is the axis of rotation symmetry. In an infinite sample, from the point of

view of the Frank-Oseen model, there is no mechanism and no typical length to keep r_{\perp} from becoming a zero; when $r_{\perp} \rightarrow 0$, the energy per unit length of the string attains its minimum value $4\pi K$ [54]. As the director gradients diverge at the core for $r_{\perp} \rightarrow 0$, a more refined approach is needed. Penzenstadler and Trebin [47] considered the Landau-de Gennes theory in which the high density of director distortions is relaxed by changing the uniaxial orientational order into the biaxial one, in the spirit of Lyuksyutov's approach to the problem of the singular core of disclinations and point defects [41,46]. They demonstrated that the soliton can decay into a uniform director structure $\mathbf{n}=\text{const}$ by a mechanism of *escape to biaxiality* [47]. However, the decay might be prevented by the energy barrier separating the uniform state from the soliton state. A stabilization mechanism has been found by Semenov [54], who added a 4th-order gradient term to the standard 2nd order Frank-Oseen functional, $f_{Fr} = \frac{K}{2}(\nabla\mathbf{n})^2 + K\xi^2(\nabla\mathbf{n})^2$. This term prescribes the soliton string to be of a (generally macroscopic) fixed radius determined by the separation distance L between the point defects located at $z = \pm L/2$ and the nematic coherence length ξ (of the order of a molecular size), namely, $r_{\perp}(z) \sim \sqrt{\xi L (1 - 4z^2 / L^2)}$. The attraction force between the defects acquires a small correction term [54], $f = -4\pi K \left(1 + \frac{3}{\sqrt{2}} \frac{\xi}{L} \sqrt{\ln \frac{L}{\xi}} \right)$.

Fig.4. Schematic director configuration of the hedgehog pair connected by a soliton string.

Any realistic liquid crystal sample is bounded; the consideration above then might be applicable only when the characteristic size R of the system is much larger than L . When the two are comparable, the theory should take into account the boundary conditions, namely, the "anchoring" direction and energy associated with the director alignment at the bounding surfaces. In addition to R , the new macroscopic length scale is K/W , usually ranging $0.01 \mu\text{m}$ to $10 \mu\text{m}$. The problem becomes much more complicated and the existing models of the offer conflicting views even for the simplest geometry of a bounded sample, such as the circular capillary depicted in Fig.1. Semenov's theory [54] and the numerical analysis by Gartland et al. [55] predict that the attraction of a pair of points in the capillary can still be described by the expression above but only when L very short, much shorter than $L^* \sim d_c^{2/3} \xi^{1/3}$ that depends on the capillary diameter d_c ; for $L > d_c$, the attractive force decreases exponentially as $\exp(-6.6L/d_c)$, setting the hedgehogs "asymptotically free" and non-interactive at large separations. Qualitatively, the bounding surface sets the director field

1
2
3 practically the same on the both sides of each defect core which implies that there is no net
4 force acting on the defect. Peroli and Virga [56] also predicted an attractive potential, but of a
5 different type: the attractive force varies logarithmically with L at short distances and
6 vanishes at $L \geq 1.1d_c$. Finally, a model by Vilfan et al. [57] predicted that the defects would
7 attract only when $L < 0.1d_c$ and repel if set at a larger separations. This last model has been
8 inspired by an experimental NMR evidence that in very narrow (submicron) cylindrical
9 cavities, there might exist a (metastable) state with alternating radial and hyperbolic
10 hedgehogs separated by $L \approx d_c$ [58]; see also the numeric simulations in Ref. [59]. Although
11 all models dealt with the same basic director geometry, the boundary conditions have been
12 chosen a bit differently, which might explain the discrepancies, according to Holyst and
13 Oswald [60]: the surface anchoring was assumed to be infinitely strong, $W \rightarrow \infty$, thus rigidly
14 fixing the director orientation at the boundary in Ref. [54], but was taken finite in Ref. [57],
15 thus allowing for the (small) director deviations from the anchoring direction at the surface.
16
17

18
19 Experimentally, the interaction of the topological point defects can be studied in
20 dynamical settings, by studying whether and how the defects of opposite topological charge
21 would attract each other and annihilate. As the first example, consider two point defects in an
22 infinitely large sample, connected by a string of a constant width r whose elastic energy per
23 unit length is $\sim K$. When the two defects approach each other, the director reorientation and
24 thus energy dissipation take place mostly in the region of size $\sim r$; the drag force acting on the
25 defects moving with the closing velocity $v \sim -dL/dt$ is then $\sim \gamma_1 r v$, where γ_1 is the viscosity
26 coefficient for director reorientations. By equating this force to the elastic force $\sim K$, one
27 concludes that the two defects should approach each other with a constant velocity; or,
28 equivalently, that the distance between the defects decreases linearly with time:
29
30

$$31 \quad L(t) \propto t_0 - t, \quad (10)$$

32
33 where t_0 denotes the moment of annihilation. Interestingly, when the soliton width tends to
34 zero, $r_{\perp} \rightarrow 0$, as in the case of infinitely large system with two point defects, then the energy
35 dissipation rate should diverge to infinity; as the elastic force remain constant, it means
36 $v \rightarrow 0$ [61]. Pismen and Rubinstein [61] interpret this result as an indication that the local
37 reduction of the uniaxial nematic order in the core region is essential for the defect interaction
38 and dynamics and deduced that the distance changes as
39
40

$$41 \quad L(t) \propto \sqrt{t_0 - t}. \quad (11)$$

1
2
3
4
5
6
7
8
9
10
11
12
13
14
15
16
17
18
19
20
21
22
23
24
25
26
27
28
29
30
31
32
33
34
35
36
37
38
39
40
41
42
43
44
45
46
47
48
49
50
51
52
53
54
55
56
57
58
59
60

The dynamics obviously change when the potential of interaction changes. For example, if the interaction potential is of a logarithmic type $\sim \ln L / \xi$ (which is the case, for example, of point defects in 2D or straight parallel disclinations in 3D [62]), then the elastic force is $\sim -1/L$ and the drag force is $\sim \gamma_1 v \ln L / \xi$; therefore, the defects move with acceleration and $L(t) \propto \sqrt{t_0 - t}$, or, including the logarithmic correction, $L^2 \left(\ln \frac{L}{\xi} + const \right) \propto t_0 - t$, still similar to Eq. (11).

The dependence $L(t) \propto t_0 - t$ for the situation when the defects are indeed connected by an experimentally observable linear soliton of a constant width, over which the director experiences a rotation by 2π (similarly to Fig.4, but not axially symmetric) has been confirmed for the pairs of boojums at the surface of the hybrid aligned nematic films [21,63] and for the defects in freely suspended SmC films [64]. The stability of the soliton requires some “ordering field” [64] (e.g., an in-plane electric field [63] or a film thickness gradient [65]) to confine the director distortions within a region of a constant width. When the solitons do not exist, and the director distortions spread in the entire region between the defects, the dynamics trend changes from Eq.(10) to Eq.(11), as observed in the experimental situations [21,63,64] above and in the hybrid aligned films of thermotropic nematic polyesters with boojums [22]. Even when the solitons connecting the point exist, one can observe a crossover from $L(t) \propto t_0 - t$ to $L(t) \propto \sqrt{t_0 - t}$ when the separation distance shrinks and becomes smaller than the width of the soliton, at the late stages of annihilation [63].

The experimental situation with the point defects in circular capillaries is even more complex. Both dependencies above have been observed for annihilating pairs of hyperbolic and radial hedgehogs produced by the isotropic-to-nematic quench in circular capillaries with $d_c = 350 \mu m$ [19]: $L(t) \propto t_0 - t$ for $L \geq d_c$ and $L(t) \propto \sqrt{t_0 - t}$ for $L \leq d_c$. A similar experiment [66] with $60 \mu m \leq d_c \leq 150 \mu m$ performed for a similar thermotropic cyanobiphenyl nematic material produced a different result: The sufficiently separated pairs $L \geq d_c$ of hyperbolic and radial hedgehogs at the axis of the capillary did not show any signs of interaction; their separation remained fixed for many hours. Once set in motion by an external perturbation such as temperature gradient along the cylinder, the defects approach each other, first with $L(t) \propto t_0 - t$ when $L \geq d_c$ and with $L(t)$ exponentially vanishing at the final stages of annihilation [66]. This is in contrast to the experiment [19] where the

1
2
3 hedgehogs were observed to approach each other even when separated by $L \approx 6d_c$, with a
4
5 constant velocity, Eq.(10), which was interpreted as the result of an elastic interaction with a
6
7 constant force $\sim K$. On the other hand, the experimental technique used by Pargellis et al [19]
8
9 to produce the defects, namely a fast temperature or pressure quench, might have led to
10
11 temperature gradients capable of setting the hedgehogs into motion even in the absence of
12
13 such an interaction. For example, the temperature difference on the two sides of a hedgehog
14
15 would cause a difference in the Frank elastic constants and thus in the elastic energies of these
16
17 two regions. Hilling and Saupe, see Ref. [67], also find $L(t) \propto t_0 - t$ for $L \geq d_c$. However,
18
19 Ref. [67] interprets it as the result of the imperfection in the normal alignment at the
20
21 cylindrical wall rather as the result of any proper elastic interaction between the defects which
22
23 was taken as non-existent for $L \geq d_c$. To illustrate the point, consider Fig.1 and assume that
24
25 the director at the boundary slightly deviates from the perpendicular orientation, by an angle
26
27 φ , say, downwards, so that the director ticks at the right boundary in Fig.1 turn from 3
28
29 o'clock towards 4 o'clock and the ticks at the left boundary turn from 9 o'clock towards 8
30
31 o'clock. Such a deviation might quite naturally be induced by the flow of the nematic fluid
32
33 during the capillary filling. Then the elastic energy (per unit length) of the configuration that
34
35 escapes "downwards" (between the two defect cores in Fig.1) will be larger than the energy
36
37 and "upward" escape (outside the defect pair), as the director rotate by $\pi + 2\varphi$ across the
38
39 capillary in the first case and by $\pi - 2\varphi$ in the second case. The energy of the escaped
40
41 configuration scales as $\sim K$ (it is independent of d_c [4]) and so does the difference in the
42
43 elastic energies (per unit length) of the two regions. Therefore, the defects would approach
44
45 each other to reduce the length of the "overdistorted" region and the dynamics should follow
46
47 Eq.(10) [67]. By reversing the sign of φ , the same argument should see the two defects in
48
49 Fig.1 moving in opposite direction: the two would repel each other rather than attract [67]. It
50
51 might be of interest to verify this feature in experiments by establishing the polarity of the
52
53 director tilt with respect to the polarity of the hedgehog pair(s).

52 To conclude, the only relatively well established experimental result for a pair of
53
54 hedgehogs in circular capillaries is that at short distances, $L \leq d_c$, their dynamics can be
55
56 described by Eq.(11) (as also confirmed in numerical simulations with the Lebwohl-Lasher
57
58 lattice model [68]). What happens at $L \geq d_c$ is not entirely clear. Recently, Holyst and
59
60 Oswald [60] proposed to use a somewhat different geometry, a set of hedgehogs at the
singular disclination line that forms near a cylindrical meniscus of a nematic sample in

1
2
3 contact with air. Subsequent experiments left the group “certain that “+1” and “-1” defects
4 attract each other over at short distances and repel at large distances” [69]. Note that all the
5 experiments performed so far reduced to the passive observations of defects locations and
6 their change in time; in the future, it might be useful to add a new experimental technique of a
7 controlled trapping and manipulating the defects with optical tweezers, see, e.g., [70,71].
8
9

10
11 An important feature of the hedgehog dynamics at short separation distances
12 established by Cladis and Brandt [66] is that the radial and hyperbolic hedgehogs move
13 towards each other in the capillary with different velocities, the former moving noticeably
14 faster than the second one, especially near the nematic-to-smectic transition, where the bend
15 deformations characteristic for the hyperbolic defect become accompanied by a very large
16 elastic constant. The result is most probably related to the backflow effect, i.e. the flow of the
17 nematic fluid caused by director reorientation. Although the backflow effect is of certain
18 importance in any defect dynamics problem, it is extremely difficult to incorporate into the
19 models and is usually neglected. Nevertheless, Blanc et al. [72] recently demonstrated that in
20 the similar problem of dynamics of two linear disclinations, the difference in the velocities of
21 the defects of different strength is related to the backflow effect rather than to the elastic
22 anisotropy.
23
24
25
26
27
28
29
30
31
32

33 The dynamics of defects has been attracted interest also from the point of view of the
34 phase transitions scenarios, not only in liquid crystals and condensed matter, but also in
35 cosmological models (the Kibble model and Zureck model, for example [73]). During the
36 quench from the highly symmetric phase (such as the isotropic fluid) to the lower symmetry
37 phase (a uniaxial nematic, for example), the different pieces of the new phase might acquire
38 different values of the order parameter phase (the director orientation) [4]; when they expand
39 and meet each other, these differences produce topological defects. The quench is then
40 followed by a relaxation process in which the density N of defects decreases as the result of
41 their annihilation; for the hedgehogs, the rule should be $N(t) \propto L^{-D}$, in D -dimensional space,
42 see, e.g., [74,75]. The isotropic-to-nematic transition has attracted especial interest in this
43 regard [15,76], mostly because of the (apparent) ease with which the experimental data can be
44 created and collected. The latest theoretical result predicts that in 3D, the hedgehog densities
45 should decay as $N(t) \propto L^{-3} \propto t^{-3/2}$ if there are no other defects such as disclinations. In the
46 experiments by Chuang et al. [15], however, the number of hedgehogs has been observed first
47 to increase immediately after the quench, then reach a maximum and quickly decrease,
48 approximately as $N(t) \propto t^{-3}$. These unusual features might be related to the presence of
49
50
51
52
53
54
55
56
57
58
59
60

disclinations and to the mutual transformations of hedgehogs and disclination rings. A direct hedgehog-hedgehog annihilation in the 3D nematic bulk without disclination lines involved has been reported to obey Eq.(11) [77]. The same behaviour (11) with $N(t) \propto L^{-2}$ has been observed by Dierking et al. [78] for the annihilation dynamics of umbilic defects in 2D. A single umbilical defect represents a pair of two surface defects-boojums on the opposite sides of the flat cell filled with the nematic of a negative dielectric anisotropy; they appear when a strong electric field is applied to the cell and the director realigns from its original homeotropic orientation. As in the case with the pair annihilation in a cylindrical capillary, much more needed to be done before the dynamics of defect tangles in quenched systems with hedgehogs and disclinations can be completely understood. Note that for the clarification of the role of backflow effect the studies of dynamics of boojums and umbilics might be very productive: the singular (molecular) core that creates problem in many computer simulations does not exist here, as the “cores” of the surface defects and umbilics are macroscopic.

3. Singular points in nematic colloidal suspensions

Colloids in which the liquid crystal is either a dispersed component [79] or nematic colloids in which the liquid crystal serves as a medium containing droplets of water or solid particles [80,81], are populated by point defects whenever the surface anchoring at the interfaces is strong enough ($R \gg K/W$). Different boundary conditions (director normal to the interface, tangential, or tilted) lead to two different types of point defects. For example, the equilibrium state of a spherical nematic droplet with normal orientation corresponds to a radial hedgehog (or its topological equivalent such as a ring), while tilted or tangential orientation lead to boojums (surface defects), Fig.5.

Fig. 5: Experimental textures of radial (a) and twisted bipolar nematic droplets (b) viewed between two crossed polarizers.

The topological characteristics of all point defects in a single connected nematic volume must satisfy the restrictions imposed by the Euler-Poincaré and Gauss theorems. For p hedgehogs and q boojums enclosed by a surface of an Euler characteristic E , the restrictions write [20]

$$\sum_{i=1}^{q+p} N_i = E/2; \quad \sum_{j=1}^p k_j = E. \quad (12)$$

1
 2
 3 The conservation laws given by Eqs. (12) can influence the late stages of the first-
 4 order isotropic-to-nematic phase transition that occurs through nucleation of nematic droplets.
 5 The droplets grow by adding molecules from the surrounding isotropic matrix and by
 6 coalescence. At early stages, the droplets are small and the director within them is practically
 7 uniform; they might form defects upon coalescence according to the Kibble mechanism, when
 8 three or more nematic droplets with different director orientation coalesce. However, as soon
 9 as the droplets grow above $R_c = K/W$, each of them acquires topological defects obeying
 10 Eq.(12). For the popular nematic pentylcyanobiphenyl (5CB), the surface anchoring
 11 coefficient at the nematic-isotropic interface is $W \approx 10^6$ J/m² [82] while $K \approx 2 \times 10^{12}$ J/m² [83];
 12 therefore the anchoring-induced production of defects becomes effective for $R \geq R_c \approx 2 \mu\text{m}$.
 13 Figure 6 shows nematic droplets growing from the isotropic melt (E7 mixture containing
 14 cyanobiphenyls, similar to 5CB): supramicron droplets clearly carry stable topological
 15 defects. Because of the surface anchoring that sets tilted conical director orientation (similar
 16 to 5CB, see [82]) there are both boojums and disclination loops [20]. As Fig.6 demonstrates,
 17 the anchoring mechanism is extremely effective, producing one disclination loop per each
 18 nematic "bubble" of the appropriate size. Bowick et al. [84] expanding on the earlier studies
 19 by Chuang et al. [15], have discovered that the number of "strings" (disclinations) produced in
 20 the isotropic-nematic transition is about 0.6 per nematic "bubble" (droplet). Although this
 21 number has been found to be in reasonable agreement with the Kibble mechanism [84], it
 22 might also signal a significant contribution from the anchoring mechanism, as many droplets
 23 in the experiment [84] have been larger than $10 \mu\text{m}$. The balance of Kibble and anchoring
 24 mechanisms in defect production during the isotropic-nematic phase transition is still an open
 25 problem. Clearly, it should strongly depend on the speed and depth of quenching; fast quench
 26 that produces numerous sub-micron nuclei separated by submicron distances might avoid the
 27 anchoring mechanism. The critical radius of nucleation is (see, for example, [4])
 28 $\rho_c = 2\sigma/f$, where $\sigma \sim 10^{-5}$ J/m² [82] is the surface tension coefficient for the isotropic-
 29 nematic interface, and f is the bulk energy density difference between the isotropic and
 30 nematic phases. Estimating $f \sim \Delta T \Delta H / T_{IN}$, where $\Delta T = T_{IN} - T$ is the depth of temperature
 31 quench and $\Delta H \sim 10^5$ J/m³ is the latent heat of transition [85], one finds the critical radius
 32 ranging from $\rho_c \sim (0.01 - 0.1) \mu\text{m}$ when the quench is a 1-10 degrees below T_{IN} and to
 33 $\rho_c \rightarrow \infty$ when $T \rightarrow T_{IN}$. Therefore, even a fast temperature quench might lead to large
 34 droplets if it is not deep enough. On the other hand, slow quench might tell a story of
 35
 36
 37
 38
 39
 40
 41
 42
 43
 44
 45
 46
 47
 48
 49
 50
 51
 52
 53
 54
 55
 56
 57
 58
 59
 60

1
2
3 anchoring-induced defect dynamics in growing droplets that is of interest on its own,
4
5 irrespective of the Kibble mechanism.
6

7 In the nematic droplets, the equilibrium director configuration and the corresponding
8 defects change when the boundary conditions change; for example, one can cause
9 transformations between bipolar structure with a pair of boojums and a hedgehog by changing
10 the temperature of the sample which in its turn changes the surface orientation from tangential
11 to normal [20,86]. Director deformations associated with the defect structures in the droplets
12 can cause flexoelectric polarization that contributes to electrostatic interactions between the
13 nematic droplets [87,88,89].
14
15
16
17
18

19 Point defects help to stabilize the nematic emulsions [90]. For example, imagine an
20 isotropic (say, water) droplet with a normal boundary conditions (that can be set by adding a
21 small amount of a surfactant such as lecithin to the system) in the nematic sample with a
22 uniform director. If the droplet is large, then it would distort the director around itself acting
23 as a radial hedgehog with an enlarged “core”. If the far-field of the director is uniform, then
24 such a droplet would create a satellite hyperbolic hedgehog that balances the topological
25 charge $N = 1$ of the droplet. The director field around the droplet adopts a dipole
26 configuration. When there are many droplets in the system, they attract each other at large
27 distances and repel at distances comparable to the droplet diameter $2R$ and thus form chains
28 of alternating droplets and hyperbolic hedgehogs. For distances $d \gg 2R$, the elastic force of
29 attraction scales as $F \propto KR^4/d^4$ [90], which has been experimentally verified for the case of
30 ferrofluid droplets [91] and most recently for solid particles manipulated by optical tweezers
31 in the nematic bulk [71,92].
32
33
34
35
36
37
38
39
40
41

42 A spectacular illustration of the role of point defects and the critical size $R_c \approx K/W$
43 in stabilization of emulsions has been found by Loudet et al [93] who demonstrated that small
44 isotropic oil droplets phase separating from the nematic host E7, can grow till their radius
45 approaches $R_c \approx 2 \mu m$; after that, each oil drop forms a satellite hyperbolic hedgehog; the
46 droplets attract each other into long chains parallel to the alignment direction of the nematic
47 phase. Ultimately, a highly ordered array of parallel macroscopic chains is formed, made of
48 monodisperse droplets which do not coalesce, in sharp contrast to the scenarios of phase
49 separation in isotropic fluids. Note that the distortions around the droplets can drive them to
50 accumulate in specific regions of the nematic matrix such as other defects (disclinations) [94]
51 and interfaces [95,96].
52
53
54
55
56
57
58
59
60

1
2
3
4
5
6
7
8
9
10
11
12
13
14
15
16
17
18
19
20
21
22
23
24
25
26
27
28
29
30
31
32
33
34
35
36
37
38
39
40
41
42
43
44
45
46
47
48
49
50
51
52
53
54
55
56
57
58
59
60

If the role of the surface anchoring is reduced (or if the electric field is applied to the droplet [97,98]), the hyperbolic hedgehog can be transformed into an equatorial disclination loop embracing the droplet, which is known as the Saturn-ring configuration, first envisioned theoretically in [99] on the basis of Frank-Oseen theory; and then observed experimentally in thermotropic [100,101] as well as lyotropic nematics [102], Fig. 7. Computer simulations also suggest that the hyperbolic hedgehog can transform into the Saturn ring when the size of the spherical particle decreases [103,104]. The interparticle interactions acquire a quadrupole symmetry when the dipole hedgehog configuration changes to that of the Saturn ring symmetry in the external electric field, as demonstrated by Loudet and Poulin [98].

The interparticle interactions become much weaker, $F \propto 1/d^6$, when the normal boundary conditions are changed to the tangential ones [105,106]. The director field acquires two defects-boojuims at the poles of the particle and the symmetry of a quadrupole. As established experimentally with the help of optical tweezers [107], the interaction might be of repulsive or attractive nature, depending on the mutual position of the two droplets, but it deviates from the quadrupolar model when the distances between the particles become comparable to a few D 's.

The studies of dynamics of defect formations in colloidal systems are at the stage of infancy [108,109]. For example, Stark and Ventzki [108] calculated the Stokes drag of spherical particles moving in a nematic host for three different configurations shown in Fig.7. The hedgehog configuration is very different from the other two because of its dipolar symmetry.

Fig. 6: The sequence of textures of nematic nuclei at the isotropic-to-nematic transition caused by temperature quench in the mixture E7 as viewed between two crossed polarizers. The nuclei carry boojuims (black arrows) and disclination loops (white arrows) (a,b); merging (c) results in disclinations with ends trapped at the cell's plates. Cell thickness 200 μm .

Fig. 7: A spherical inclusion in a uniformly aligned nematic matrix with homeotropic boundary conditions resembles a radial hedgehog and produces a hyperbolic satellite when its size is much larger than the anchoring extrapolation length K/W (a); causes a Saturn ring configuration when the two are comparable (b); and is being ineffective to distort the director when much smaller than K/W (c).

4. Conclusion

The large birefringence of liquid crystals allow easy optical microscopy observations of defects, whose number is scarce in the field of view, due to the viscous relaxation of the sample inhomogeneities; observed defects are usually in equilibrium with the boundary conditions, and of small energy. This explains why *topological point defects* in condensed matter physics were discovered there, in parallel with the investigations on Bloch points in

1
2
3 magnetic bubbles [110]. This is at the origin of a noticeable (but limited) series of
4 observations and, above all, of theoretical developments, including the topological theory of
5 defects and their elastic and dynamic properties. The present day observation resolution is far
6 below the advances made thanks to computational methods, in particular in the structure of
7 the core and the anisotropy of the Frank coefficients; new experimental methods are thus all
8 wanting. One can however expect that more recent optical methods, such as ultra rapid
9 confocal polarizing microscopy, attended by laser manipulations of small particles (*e.g.* in
10 nematic colloidal suspensions) or even of defects themselves, might help in the investigation
11 of macroscopic dynamic properties, at least.

12
13
14
15
16
17
18
19
20
21
22
23
24
25
26
27
28
29
30
31
32
33
34
35
36
37
38
39
40
41
42
43
44
45
46
47
48
49
50
51
52
53
54
55
56
57
58
59
60

ODL acknowledges useful discussions with E. C. Gartland, Jr. and partial support through NSF grants DMR-0504516 and DMS -0456221.

REFERENCES

- [1] L. Michel, *Rev. Mod. Phys.* **52** 617 (1980).
[2] H. Poincaré, *J. Math.* **2** 151(1886).
[3] F. R. N. Nabarro, *J. Physique* **33** 1089 (1972).
[4] M. Kleman and O. D. Lavrentovich, *Soft Matter Physics, an Introduction* (Springer, New York, 2003).
[5] M. Kleman, O. D. Lavrentovich, and Y. A. Nastishin in *Dislocations in Solids* edited by F. R. N. Nabarro and J. P. Hirth, **12** 150 (2005).
[6] D. Hilbert and S. Cohn-Vossen, *Geometry and the Imagination* (Chelsea Pub. Cy, New York, 1954).
[7] M. Kleman, *Philos. Mag.* **27** 1057 (1973).
[8] G. E. Volovik and V. P. Mineyev, *Zh. Eksp. Teor. Fiz.* **72** 2256 (1976) [*Sov. Phys. JETP (USA)* **45** 1186 (1977)].
[9] F. R. N. Nabarro, *Conference on Fundamental Aspects of the Theory of Dislocations*, Gaithersburg, April 1969. NBS Special Publi. **317** 593 (1970).
[10] D. Melzer and F. R. N. Nabarro, *Philos. Mag.* a)- **35** 901(1977); b)- **35** 907(1977).
[11] R. B. Meyer, *Mol. Cryst. Liq. Cryst.* **16** 355 (1972).
[12] I. Chuang, B. Yurke, A. N. Pargellis, and N. Turok, *Phys. Rev.* **E47** 3343 (1993).
[13] M. Hindmarsh, *Phys. Rev. Lett.* **75** 2502 (1995).
[14] T. W. B. Kibble, *J. Phys.* **A9** 1387 (1976).
[15] I. Chuang, R. Durrer, N. Turok, and B. Yurke, *Science* **251** 1336 (1991).
[16] C. Williams, P. Piéranski, and P. E. Cladis, *Phys. Rev. Lett.* **29** 90 (1972).
[17] A. Saupe, *Molec. Cryst. Liq. Cryst.* **21** 211 (1973).
[18] C. Williams, P. E. Cladis, and M. Kléman, *Molec. Cryst. Liquid Cryst.* **21** 355 (1973).
[19] A. Pargellis, N. Turok, and B. Yurke, *Phys. Rev. Lett.* **67** 1570 (1991).

- 1
2
3
4
5 [20] G. E. Volovik and O. D. Lavrentovich, Zh. Eksp. Teor. Fiz. **85** 1997 (1983) [Sov. Phys. JETP (USA) **58**
6 1159 (1983)].
7 [21] O. D. Lavrentovich and S. S. Rozhov, Pis'ma Zh. Eksp. Teor. Fiz. **47** 210 (1988) [Sov. Phys. JETP Lett., **47**
8 254 (1988)].
9 [22] D.-K. Ding and E. L. Thomas, Mol. Cryst. Liq. Cryst. **241** 103 (1994).
10 [23] R. B. Meyer, Philos. Mag. **27** 405 (1973).
11 [24] P. E. Cladis and M. Kleman, J. Physique **33** 591 (1972).
12 [25] S. I. Anisimov and I. Dzyaloshinskii, Sov. Phys. JETP **36** 774 (1972).
13 [26] G. Mazelet and M. Kleman, Polymer **27** 714 (1986).
14 [27] C. Chiccoli, I. Feruli, O. D. Lavrentovich, P. Pasini, S. V. Shiyonovskii, and C. Zannoni, Phys. Rev. **E66**
15 030701(R) (2002).
16 [28] S. Candau, P. Le Roy and Debeauvais, Mol. Cryst. Liq. Cryst. **23** 283 (1973).
17 [29] L.A. Madsen, T.J. Dingemans, M. Nakata, and E.T. Samulski, Phys. Rev. Lett. **92** 145505 (2004)
18 [30] B.R. Acharya, A. Primak, and S. Kumar, Phys. Rev. Lett. **92** 145506 (2004).
19 [31] G. E. Volovik, Sov. Phys. JETP Lett. **28**, 59 (1978).
20 [32] M. J. Press and A. S. Arrott, J. Physique **36** C1-177 (1975)
21 [33] H. Brezis, J.-M. Coron, and E. H. Lieb, Comm. Math. Phys. **107** 647 (1986).
22 [34] S. Ostlund, Phys. Rev. **B24** 485 (1981).
23 [35] W. F. Brinkman and P. E. Cladis, Physics Today **35** 48 (1982).
24 [36] M. J. Press and A. S. Arrott, Phys. Rev. Lett. **33** 403 (1974).
25 [37] O. D. Lavrentovich and V. V. Sergan, Nuovo Cimento, Ser. D – Cond. Matt. **12** 1219 (1990).
26 [38] R.D. Williams, J. Phys. A **19** 3211 (1984);
27 [39] P. Prinsen and P. van der Schoot, J. Phys.: Condens. Matter **16** 8835 (2004)
28 [40] F. Hélein, C. R. Acad. Sci. Paris **305** 565 (1987).
29 [41] I. F. Lyuksyutov, Zh. Eksp. Teor. Fiz. **75** 358 [Sov. Phys. JETP **48** 178 (1978)].
30 [42] H. Mori and H. Nakanishi, J. Phys. Soc. Japan **57** 1281 (1988).
31 [43] O. D. Lavrentovich, T. Ishikawa, and E. M. Terentjev, Mol. Cryst. Liq. Cryst. **299** 301 (1997).
32 [44] V.G. Bodnar, O.D. Lavrentovich, V.M. Pergamenschik, Zh. Eksp. Teor. Fiz. **101**, 111 (1991) [Sov. Phys.
33 JETP **74**, 60 (1992)]
34 [45] J.-i. Fukuda and H. Yokoyama, Phys. Rev. **E66** 012703 (2002).
35 [46] N. Schopol and T. J. Sluckin, J. Physique (France) **49** 1097 (1981).
36 [47] E. Penzenstadtler and H.-R. Trebin, J. Physique (France) **50** 1027 (1981).
37 [48] R. Rosso and E. G. Virga, J. Phys. A: Math. Gen. **29** 4247 (1996).
38 [49] N. Schopol and T. J. Sluckin, Phys. Rev. Lett. **59** 2582 (1987).
39 [50] P. Biscari, G. Guidone Peroli, and T. J. Sluckin, Mol. Cryst. Liq. Cryst. **292** 91 (1997).
40 [51] E. C. Gartland, Jr. and S. Mkaddem, Phys. Rev. **E59** 563 (1999); S. Mkaddem and E. C. Gartland, Jr., Phys.
41 Rev. **E62**, 6694 (2000).
42 [52] a)-S. Kralj, E. G. Virga, and S. Zumer, Phys. Rev. **E60** 1858 (1999); b)-S. Kralj and E. G. Virga, J. Phys.
43 A: Math. Gen. **34** 829 (2001).
44
45
46
47
48
49
50
51
52
53
54
55
56
57
58
59
60

- 1
2
3
4
5 [53] *Defects in Liquid Crystals: Computer simulations, theory and experiment* edited by O. D. Lavrentovich, P.
6 Pasini, C. Zannoni, and S. Zumer (Kluwer Academic Publishers, the Netherlands, 2001).
7
8 [54] A. N. Semenov, Europhys. Lett. **46** 631 (1999)
9
10 [55] E.C. Gartland, Jr., A.M. Sonnet, E.G. Virga, Continuum Mech. Thermodyn. **14**, 307 (2002)
11 [56] G. Guidone Peroli and E. G. Virga, Phys. Rev. **E54** 5235 (1996); **56**, 1819 (1997).
12 [57] I. Vilfan, M. Vilfan, and S. Zumer, Phys. Rev. **A43** 6875 (1991)
13 [58] G.P. Crawford, M. Vilfan, J.W. Doane, I. Vilfan, Phys. Rev. **A 34**, 835 (1991)
14 [59] Z. Bradac, S. Kralj, S. Zumer, Phys. Rev. E **58**, 7447 (1998)
15 [60] R. Holyst and P. Oswald, Phys. Rev. **E65** 041711 (2002).
16 [61] L. M. Pismen and B. Y. Rubinstein, Phys. Rev. Lett. **69** 96 (1992).
17 [62] Y.A. Dreizen, A.M. Dykhne, Sov. Phys. JETP **34**, 1140 (1972).
18 [63] K. Minoura, Y. Kimura, K. Ito, R. Hayakawa, and T. Miura, Phys. Rev. **E 58**, 643 (1998).
19 [64] A.N. Pargelis, P. Finn, J.W. Goodby, P. Panizza, B. Yurke and P.E. Cladis, Phys. Rev. **A 46**, 7765 (1992)
20 [65] D.R. Link, M. Nakata, K. Ishikawa, H. Takezoe, Phys. Rev. Lett. **87**, 195507 (2001)
21 [66] P. E. Cladis and H. R. Brand, Physica A **326** 322 (2003).
22 [67] G. G. Peroli, G. Hilling, A. Saupe, and E.G. Virga, Phys. Rev. E **58**, 3259 (1998)
23 [68] M. Svetec, Z. Bradac, S. Kralj, and S. Zumer, Mol. Cryst. Liq. Cryst. **413**, 43 (2004)]
24 [69] A. Zywockinski, K. Pawlak, R. Holyst, P. Oswald, J. Phys. Chem. B **109**, 9712 (2005).
25 [70] J.-I. Hotta, K. Sasaki, H. Masuhara, Appl. Phys. Lett. **71**, 2085 (1997)
26 [71] I.I. Smalyukh, A.N. Kuzmin, A.V. Kachynski, P.N. Prasad, and O.D. Lavrentovich, Appl. Phys. Lett. **86**
27 021913 (2005).
28 [72] C. Blanc, D. Svensek, S. Zumer, and M. Nobili, Phys. Rev. Lett. **95**, 097802 (2005).
29 [73] *Patterns of Symmetry Breaking* edited by H. Arodz, J. Dziarmaga and W.H. Zurek (Kluwer Academic
30 Publishers, the Netherlands, 2003).
31 [74] H. Toyoki, Phys. Rev. **A 42**, 911 (1990).
32 [75] R.A. Wickham, Phys. Rev. E **56**, 6843 (1997)
33 [76] M. J. Bowick, L. Chandar, E. A. Schiff and A. M. Srivastava, Science **263** 943 (1994).
34 [77] A.N. Pargellis, J. Mendez, M. Srinivasarao, B. Yurke, Phys. Rev. E **53**, R25 (1996).
35 [78] I. Dierking, O. Marshall, J. Wright, and N. Bulleid, Phys. Rev. E **71**, 061709 (2005).
36 [79] P.S. Drzaic, *Liquid Crystal Dispersion* (World Scientific, Singapore, 1995).
37 [80] H. Stark, Physics Reports **351**, 387 (2001).
38 [81] P. Poulin, Curr. Opin. Colloid & Interf. Sci. **4**, 66 (1999).
39 [82] S. Faetti, V. Palleschi, Phys. Rev. **A 30**, 3241 (1984).
40 [83] M.J. Bradshaw, E.P. Raynes, J.D. Bunning, T.E. Faber, J. Physique **46**, 1513 (1985).
41 [84] M.J. Bowick, L. Chandar, E.A. Schiff, A.M. Srivastava, Science **263**, 943 (1994).
42 [85] H. Yokoyama, J. Chem. Soc. Faraday Trans. **2**, 84 (1988).
43 [86] O.O. Prishchepa, A.V. Shabanov, V. Y. Zyryanov, Phys. Rev. E **72**, 031712 (2005).
44 [87] R.B. Meyer, Phys. Rev. Lett. **22** 918 (1969).
45 [88] O.D. Lavrentovich, Pis'ma Zh. Tekh. Fiz. **14**, 166 (1988) /Sov.Tech.Phys.Lett. **14** 73 (1988).
46 [89] N.M. Golovataya, M.V. Kurik, and O.D. Lavrentovich, Liq. Cryst. **7**, 287 (1990).
47
48
49
50
51
52
53
54
55
56
57
58
59
60

- 1
2
3
4
5 [90] P. Poulin, H. Stark, T.C. Lubensky, and D.A. Weitz, *Science* **275**, 1770 (1997); T.C. Lubensky, D. Pettey,
6 N. Currier, H. Stark, *Phys. Rev. E* **57**, 610 (1998); P. Poulin, D.A. Weitz, *Phys. Rev. E* **57**, 626 (1998).
7 [91] P. Poulin, V. Cabuil, and D.A. Weitz, *Phys. Rev. Lett.* **79**, 4862 (1997).
8 [92] M. Yada, J. Yamamoto, H. Yokohama, *Phys. Rev. Lett.* **92**, 185501 (2004)
9 [93] J.-C. Loudet, P. Barois, and P. Poulin, *Nature* **407**, 611 (2000).
10 [94] D. Voloschenko, O.P. Pishnyak, S.V. Shiyonovskii, O.D. Lavrentovich, *Phys. Rev. E* **65**, 060701 (R) (2002)
11 [95] J.L. West, K. Zhang, A.V. Glushchenko, Y. Reznikov, D. Andrienko, *Mol. Cryst. Liq. Cryst.* **422**, 73 (2004)
12 [96] M. Mitov, F. De Guerville, C. Bourgerette, *Mol. Cryst. Liq. Cryst.* **435**, 673 (2004)
13 [97] H. Stark, *Eur. Phys. J. B* **10**, 311 (1999) ; *Phys. Rev. E* **66**, 032701 (2002).
14 [98] J.C. Loudet, P. Poulin, *Phys. Rev. Lett.* **87**, 165503 (2001)
15 [99] O.V. Kuksenok, R.W. Ruhwandl, S.V. Shiyonovskii, E.M. Terentjev, *Phys. Rev. E* **54**, 5198 (1996); S.V.
16 Shiyonovskii and O.V. Kuksenok, *Mol. Cryst. Liq. Cryst. A* **321**, 489 (1998).
17 [100] Y. Gu and N.L. Abbott, *Phys. Rev. Lett.* **85**, 4719 (2000).
18 [101] J.C. Loudet, O. Mondain-Monval, P. Poulin, *Eur. Phys. J. E* **7**, 205 (2002).
19 [102] O. Mondain-Monval, J.C. Dedieu, T. Gulik-Krzywicki, P. Poulin, *Eur. Phys. J. B* **12**, 167 (1999)
20 [103] A.-i. Fukuda, M.; Yoneya, H. Yokoyama, *Phys. Rev. E* **65**, 041709 (2002).
21 [104] D. Andrienko, G. Germano, M.P. Allen, *Phys. Rev. E* **63**, 041701 (2001).
22 [105] S. Ramaswamy, R. Nityananda, V. Raghunathan, and J. Prost, *Mol. Cryst. Liq. Cryst.* **228** 175 (1996).
23 [106] R.W. Ruhwandl and E.M. Terentjev, *Phys. Rev. E* **55** 2958 (1997).
24 [107] I.I. Smalyukh, O.D. Lavrentovich, A.N. Kuzmin, A.V. Kachynski, and P.N. Prasad, *Phys. Rev. Lett.* **95**,
25 157801 (2005).
26 [108] H. Stark and D. Ventzki, *Phys. Rev. E* **64**, 031711 (2001).
27 [109] J.-i. Fukuda, H. Stark, H. Yokoyama, *Phys. Rev. E* **72**, 021701 (2005).
28 [110] A. P. Malozemoff and J. C. Slonczewski, *Magnetic Domain Walls in Bubble Materials* (Academic Press,
29 New York, 1979).
30
31
32
33
34
35
36
37
38
39
40
41
42
43
44
45
46
47
48
49
50
51
52
53
54
55
56
57
58
59
60